# INVERSE MODELING TO PREDICT EFFECTIVE LEAKAGE AREA

A Thesis
Presented to
The Academic Faculty

by

TE QI

In Partial Fulfillment
of the Requirements for the Degree
Master of Science in the
School of Architecture

Georgia Institute of Technology
December 2012

# INVERSE MODELING TO PREDICT EFFECTIVE LEAKAGE AREA

Approved by:

Dr. Godfried Augenbroe, Advisor
School of Architecture
*Georgia Institute of Technology*

Dr. Sang Hoon Lee
School of Architecture
*Georgia Institute of Technology*

Date Approved: November ,2012

# ACKNOWLEDGEMENTS

I would like to thank my academic advisor, Professor Augenbroe, without whom I can’t accomplish what I have done during my Master study. His continued support, invaluable suggestions, and guidance help me pass through many difficulties during this research. Thank you so much not only because of the knowledge you convey, but also the personality you have that affects me to be more confident and positive.

I would also like thank the Energy Efficiency Hub, where I spent an amazing summer doing research about this infiltration analysis as a summer intern. Specially thanks Wagner, Timothy C and O'Neill, Zheng D, who gave me excellent guidance about this research.

I would like to take this opportunity to thank all the friends I came across during the one and half year study in Atlanta, thanks all your guys to let me have a wonderful life here with an unforgettable memory.

Finally, I am deeply grateful to my family for inspiring me to further my education and loving me all the time.

# TABLE OF CONTENTS

# LIST OF TABLES

Page

# LIST OF FIGURES

# SUMMARY

The purpose of this research is to develop a new approach to estimate the effective leakage area using the inverse modeling process as an alternative to the blower door test. An actual office building, which is the head quarter of Energy Efficiency Hub, was used as an example case in this study.

The main principle of the inverse modeling process is comparing the real monitor boiler gas consumption with the result calculated from the EnergyPlus model with a dynamic infiltration rate input to find the best estimation of the parameter of effective leakage area (ELA). This thesis considers only the feasibility of replacing the blower door test with the calibration approach, so rather than attempting an automated calibration process based on inverse modeling we deal with generating a first estimate and consider the role of model uncertainties that would make the proposed method less feasible.

There are five steps of the whole process. First, we need to customize our own actual weather data (AMY) needed by the energy model (EnergyPlus model), which can help increase our quality of the result. Second, create the building energy model in EnergyPlus. Third, create a multi-zone model using CONTAM with different ELA estimation of each facade to calculate the dynamic infiltration rate of each ELA estimate. Fourth, input the dynamic infiltration rate got from the CONTAM model to EnergyPlus model and output the boiler energy consumption. Fifth, compare the boiler gas consumption from the model and the real monitor data and find the best

match between the two and the corresponding ELA, which gives the best estimate from the whole inverse modeling process.

From the simulation result comparison, the best estimation of the total building ELA from the inverse modeling process is the 23437cm$^2$ at 4pa, while the result from the blower door test is 10483cm$^2$ at 4pa. Because of the insufficient information of the building and also the uncertainty of the input parameters, the study has not led to a definite statement whether the proposed calibration of the ELA with consumption data can replace a blower door test to get an equally valid or even better ELA estimate, but it looks feasible. As this this case study is done in a deterministic context, the full feasibility test should be conducted under uncertainty. A first step towards this will be discussed in chapter 4.

# CHAPTER 1 INTRODUCTION

## 1.1 Motivation

Infiltration is the unintentional or accidental introduction of outside air into a building, typically through cracks in the building envelope and through use of doors for passage. Infiltration is sometimes called air leakage. The leakage of room air out of a building, intentionally or not, is called exfiltration. Infiltration is caused by wind, negative pressurization of the building, and by air buoyancy forces known commonly as the stack effect. In typical modern U.S. residences, about one-third of the HVAC energy consumption is due to infiltration [1]. As such, reducing infiltration can yield significant energy savings, with rapid payback. Thus in performance based building simulation processes, it is essential to estimate infiltration rates. However, due to the stochastic nature of weather, occupant's behavior, physical aspects of building components, uncertainty in simulation parameters in general, estimating natural ventilation rate is difficult [2]. There are mainly two ways of measuring building infiltration: effective leakage area (ELA) and air exchange rate per hour (ACH). This study uses ELA as the major parameter in infiltration modeling. The aggregated ELA value of a building (or different zones) could be measured with pressurization testing, commonly conducted as blower-door test operated on the building as whole. Blower-door testing is an expensive way to estimate infiltration, which stimulates us to find alternatives that are less expensive to estimate the ELA. This report is trying to estimate the ELA of the whole building through an inverse modeling process (also referred to as calibration) with a multi-zone model where we use monitored consumption data as the target of the calibration.

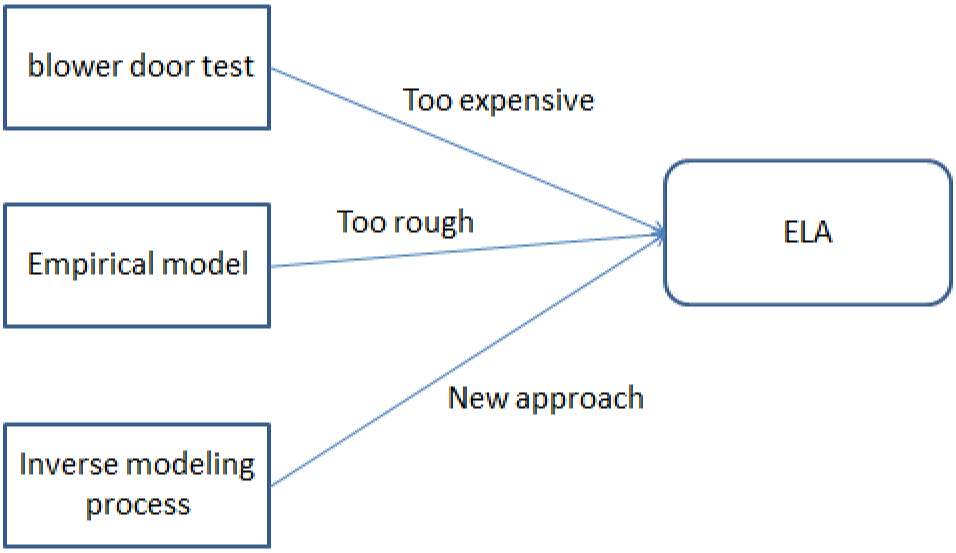


Figure 1-1 Different approach comparison

## 1.2 Background

### 1.2.1 Blower-door test approach

A building's envelope leakage can be measured with pressurization testing, commonly called a blower door test [3]. In this procedure, a large fan or blower is mounted in a door or window and induces a large and roughly uniform pressure difference across the building shell [ASTM Standards E779 and E1827; Canadian General Standards Board (CGSB) Standard 149.10; ISO Standard 9972]. The airflow required to maintain this pressure difference is the infiltration rate at a certain pressure. Thus the results of a pressurization test consist of several combinations of pressure difference and airflow rate data. An example of typical data is shown below:

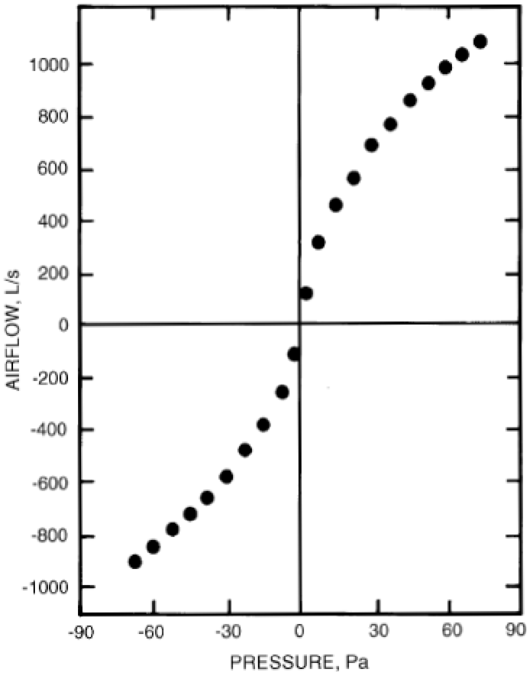

Figure 1-2 Airflow rate versus pressure difference data

Usually, the predicted airflow rate is converted to an equivalent or effective air leakage area by equation 1-1:

$$A_l = 10000Q_r\frac{\sqrt{\rho/2\Delta P_r}}{C_D} \qquad 1\text{-}1$$

where

$A_L$： equivalent or effective air leakage area, cm2;

$Q_r$： predicted airflow rate at $\Delta p_r$ (from curve fit to pressurization test data), m3/s;

$\rho$： air density, kg/m3;

$\Delta p_r$： reference pressure difference ,Pa;

$C_D$： discharge coefficient.

Some common airtightness ratings include the effective air leakage area at 4 Pa assuming Cd=1.0 (Sherman and Grimsrud 1980); the effective air leakage area at 10 Pa assuming Cd=0.611(CGSB standard 149.10).

### 1.2.2 Empirical models

When onsite blow-door test data are not available, some empirical equations could be used for a reasonable estimate. One classical infiltration model is the "Sherman-Grimsrud" model developed by Max Sherman and David Grimsrud. Equation 1-1 and Equation 1-2 show the mathematical formulas. Table 1-1 and Table 1-2 show values of two model parameters respectively: stack coefficient and wind coefficient [3].

$$\mathrm{Q} = \frac{A_L}{1000}\sqrt{C_s \Delta t + CwU^2} \qquad (1\text{-}1)$$

Where

Q airflow rate, $m^3/s$;

AL effective air leakage area, $cm^2$;

Cs stack coefficient, $(L/s)^2/(cm^2 \cdot K)$;

$\Delta t$ average indoor-outdoor temperature difference for time interval of calculation, K;

Cw wind coefficient, $(L/s)^2/[cm4 \cdot (m/s)^2]$;

U average wind speed measured at local weather station for time interval of calculation, m/s.

$$\mathrm{NL} = 0.1\left\{\frac{A_L}{A_f}\right\}\left\{\frac{H}{H_0}\right\}^3 \qquad (1\text{-}2)$$

Where

NL normalized leakage area, dimensionless;

AL effective leakage area at 4 Pa (CD=1.0), $cm^2$;

Af gross floor area (within exterior walls), $m^2$;

H building height, m;

H0 reference height of one-story building, 2.5m.

Table 1-1 Stack coefficient Cs

| | House Height | | |
|---|---|---|---|
| | one | two | three |
| Stack Coefficient | 0.000145 | 0.00029 | 0.000435 |

Table 1-2 Wind coefficient Cw

| | House height (Stories) | | | Description |
|---|---|---|---|---|
| | One | Three | Two | |
| 1 | 0.000319 | 0.000494 | 0.000420 | No obstructions or local shielding |
| 2 | 0.000246 | 0.000382 | 0.000325 | Typical shelter for an isolated rural house |
| 3 | 0.000174 | 0.000271 | 0.000231 | Typical shelter caused by other buildings across the street from the building under study |
| 4 | 0.000104 | 0.000161 | 0.000137 | Typical shelter for urban buildings on larger lots where sheltering obstacles are more than one building height away |
| 5 | 0.000032 | 0.000049 | 0.000042 | Typical shelter produced by buildings or other structures that are immediately adjacent (closer than one house height): e.g., neighboring houses on the same side of the street, trees, bushes, etc. |

### 1.2.3 Multi-zone model approach

Multi-zone models are more effective to calculate airflow, contaminant transport, heat transfer, or some combination thereof. In this case, the multi-zone flow network approach is used for trace transient infiltration rate. Network airflow models idealize a building as a collection of zones, such as rooms, hallways, and duct junction, joined by flow paths representing doors, windows, fans, ducts, etc.

The network model airflows are driven by the pressure differences across the paths. Three are three types of forces drive the airflow through airflow paths: wind, temperature differences (stack effect), and mechanical devices such as fans.

As shown below, airflow network models resemble electrical networks. Airflow corresponds to electric current, with zone pressure acting like the voltage at an electrical node. Flow paths correspond to resistors and other electrical elements, including active elements like batteries (fans) [4].

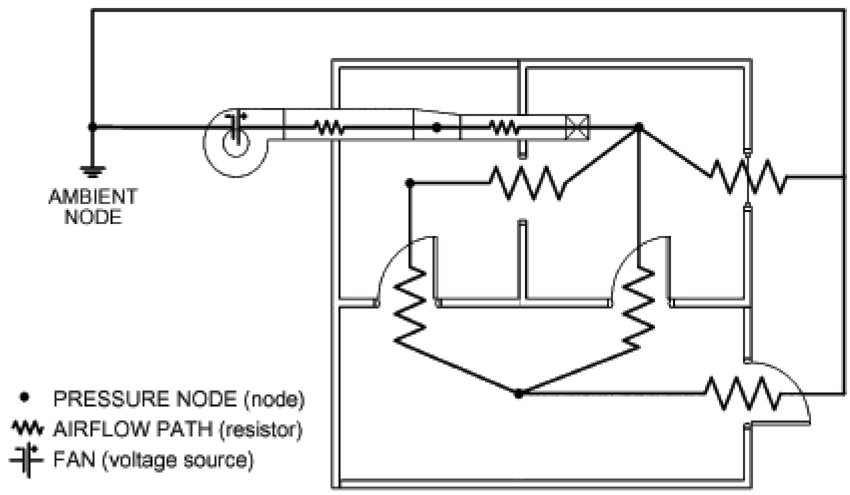


Figure 1-3 Airflow path diagram

### 1.2.4 Introduction of CONTAM

To build the multi-zone model, CONTAM was used in this case study. CONTAM is a multi-zone indoor air quality and ventilation analysis computer program designed to determine:

(1) Airflows: infiltration, exfiltration, and room-to-room airflows in building systems driven by mechanical means, wind pressures acting on the exterior of the building, and buoyancy effects induced by the indoor and outdoor air temperature difference.

(2) contaminant concentrations: the dispersal of airborne contaminants transported by these airflows; transformed by a variety of processes including chemical and radio-chemical transformation, adsorption and desorption to building materials, filtration, and deposition to building surfaces, etc.; and generated by a variety of source

mechanisms.

(3) Personal exposure: the predictions of exposure of occupants to airborne contaminants for eventual health risk assessment.

### 1.2.5 Wind pressure coefficient

Wind pressure can be a significant driving force for air infiltration through a building envelope. It is a function of wind speed, wind direction, building configuration, and local terrain effects [5].

When the wind strikes perpendicular to a building face, it creates a positive pressure on the windward building surface while results in a negative pressure on the leeward building facades. The pressure developed on the windward wall surface is not the stagnation pressure (Pu) of the wind. Instead, air slips around the sides and over the top of the building in a somewhat complicated fashion generally resulting in a surface pressure somewhat lower than the stagnation pressure [6]. A modifying factor (Cp) is used to account for the deviation between the stagnation pressure and the wind pressure at a particular point on the surface.

Stagnation Pressure $Pu = \frac{1}{2}\rho U_{ref}$

Local Pressure $(\mathrm{Px}) = \mathrm{CpPu}$

Where

Uref is the wind velocity at the point of impingement

ρ is the density of air

Cp is the local wind pressure coefficient at the point of impingement.

The wind pressure coefficient can be further generalized in terms of a local terrain effects coefficient and the direction of the wind relative to the wall under consideration. The following equation 1-3 is that used in CONTAM when calculating wind pressure on the building.

$$P_w = \frac{\rho Vmet^2}{2} C_h f(\theta) \qquad 1\text{-}3$$

where

ρ ambient air density

*Vmet* wind speed measured at meteorological station

*Ch* wind speed modifier coefficient accounting for terrain and elevation effects

f coefficient that is a function of the relative wind direction. CONTAM refers to this function as the wind pressure profile.

# CHAPTER 2 FEASIBILITY STUDY OF THE INVERSE METHOD TO ESTIMATE ELA

## 2.1 Procedure of the inverse modeling process

There are five steps of this inverse modeling process.

(1). Customize weather data

(2). Create a reliable energy model

(3). Create a multi-zone model using CONTAM with different ELA.

(4). Export the infiltration rate outcomes from CONTAM model to generate infiltration schedules in EnergyPlus

(5). Compare the results and find the best fit.

The above is a hand-crafted estimation process which is good enough for this feasibility study. In future implementations, this should become a full-blown optimization process to estimate ELA, which means that the EnergyPlus model should be able to automatically import the infiltration rate calculated from the CONTAM model of each run based on a certain ELA test value. This would allow to run the whole process in an optimization loop until the best match is found, e.g. by minimizing the total squared difference between modeled and real boiler gas consumption..

At this stage of the feasibility, and because of the complexity of the CONTAM-EnergyPlus connection in case of complex building models, this whole process was not yet automated Instead, 10 discrete ELA inputs were defined in an interval from 10905cm2 to 32343cm2 to find a reasonable approximation of the “best” estimate for ELA. In fact, this means that we test ten samples from a uniformly distributed interval of ELA and run a poor man’s Monte Carlo simulation.

System diagram:

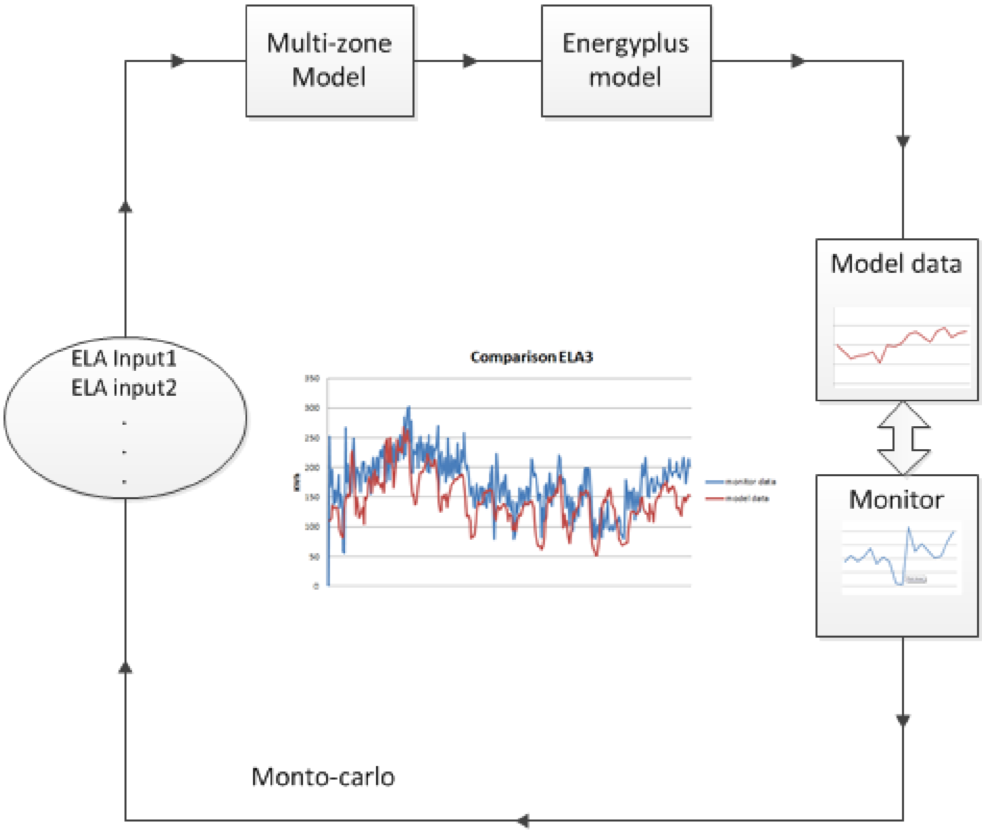


Figure 2-1 Full optimization procedure diagram

## 2.2 Introduction of the case building

Building 101 in the Navy Yard is the temporary headquarters of the U.S. Department of Energy's Energy Efficient Building Hub. The building, owned by the Philadelphia Industrial Development Corporation (PIDC), has become one of the nation's most highly instrumented commercial buildings.

Acquired data is continuously stored and is made available to Hub researchers and other building energy efficiency researchers for development, validation and calibration modeling and simulation tools, and for assessment of the impact of building energy technologies and systems on energy use.


Figure 2-2 Location of the building 101

Figure 2-3 West-view of building 101

## 2.3 Customizing weather data

Since we want to compare the result from the energy model with monitor data, it is necessary to use the actually weather data for the site and monitored period, also called AMY data, instead of typical meteorological year, also called TMY data.

A typical meteorological year (TMY) data set provides designers and other users with a reasonably sized annual data set that holds hourly meteorological values that typify conditions at a specific location over a longer period of time, such as 30 years. TMY data sets are widely used by building designers and others for modeling renewable energy conversion systems. Although not designed to provide meteorological extremes, TMY data have natural diurnal and seasonal variations and represent a year of typical climatic conditions for a location [7].

TMY data and part of the AMY weather data was downloaded from the EnergyPlus website, then the temperature, wind speed and wind direction in TMY data were replaced with the AMY data.

Since the infiltration rate will have more effects on the heating condition, a heating dominated month was selected as the simulation period, thus as the comparison period. In addition, two main factors that influence the infiltration rate are wind direction and wind speed. To try best to avoid the uncertainty of the other energy model parameter, we need to find the most fluctuate wind velocity week to analyze. Based on these considerations it was to use Jan/01 to Jan/14 as the calibration period as indicated in Figure 2-6.

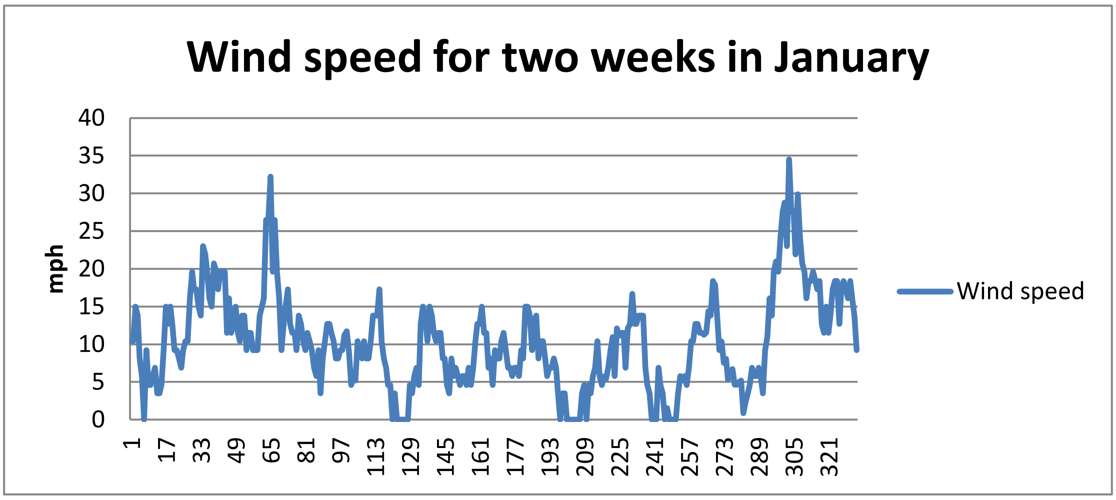


Figure 2-4 Wind speed profile from Jan/01 to Jan/14

## 2.4 Create the building energy model in EnergyPlus

In this project, EnergyPlus was selected as the energy simulation tool. At the beginning, a detailed energy model was created in design builder. However, for this particular objective of ELA estimation, to make the model complexity manageable, the model was simplified to a level that will not affect too much the final simulation result. One main reason to simplify is that the inverse modeling process cannot be accomplished automatically without making the CONTAM model fully aligned with the zones and enclosures in EnergyPlus. Keeping the zoning of the multi-zone model consistence with the energy model leads to over-engineering of the CONTAM model, which was not deemed useful for this feasibility study. As a fairly complex energy model was used to reflect the true energy behavior of the building, the flow model was based on plausible simplification in order to eliminate a lot unnecessary labor work. The figures from figure 2-7 to figure 2-15 show the building floor plans and their simplified model representations.

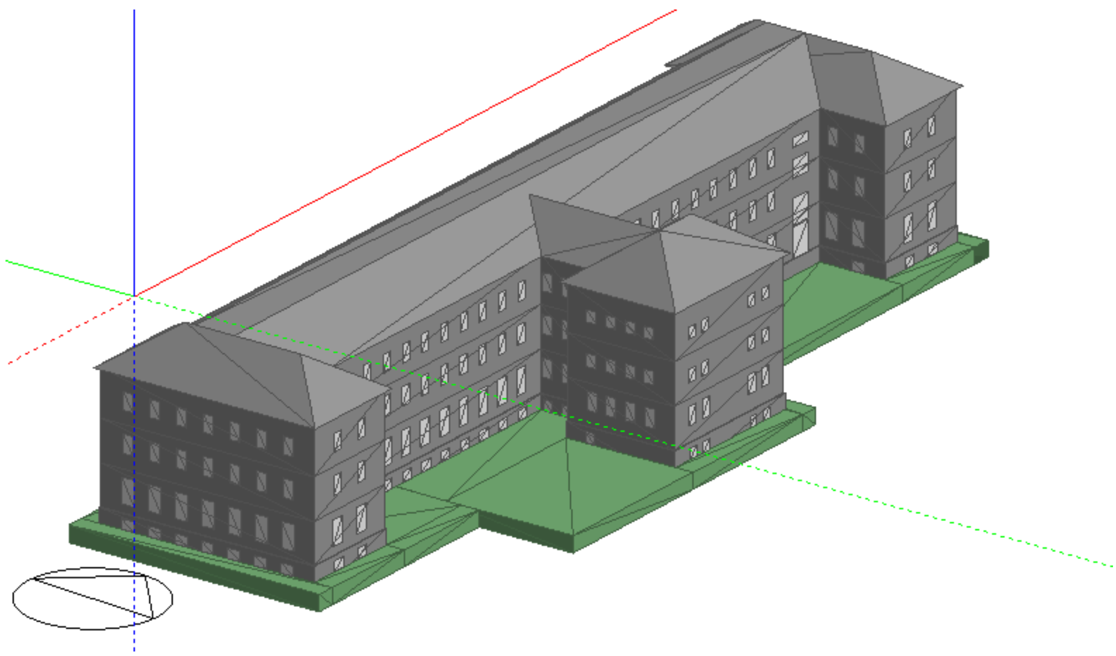

Figure 2-5 Detailed energy model

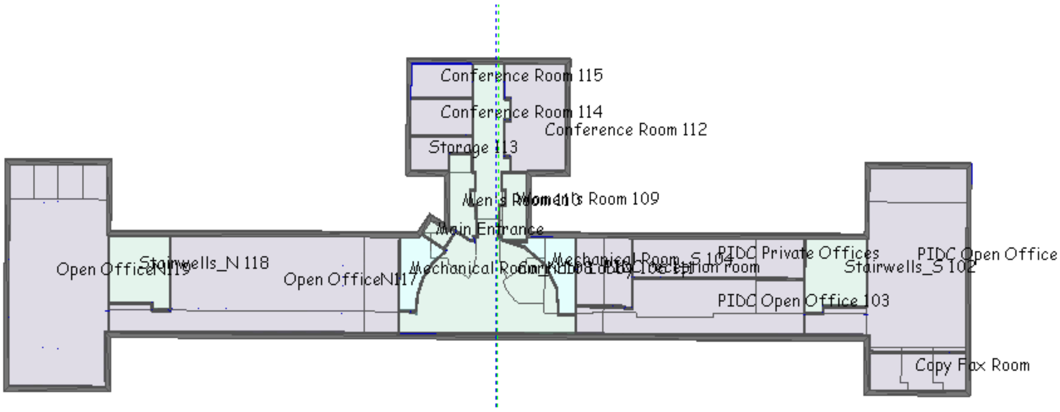


Figure 2-6 Detailed 1st floor plan

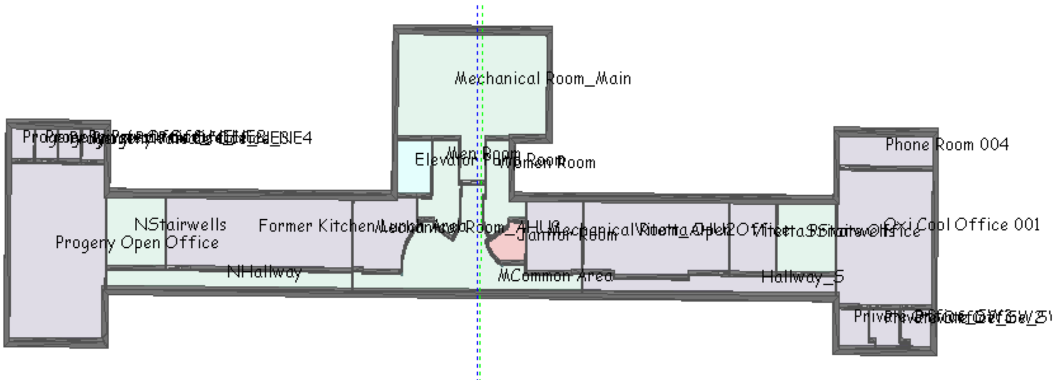


Figure 2-7 Detailed basement floor plan

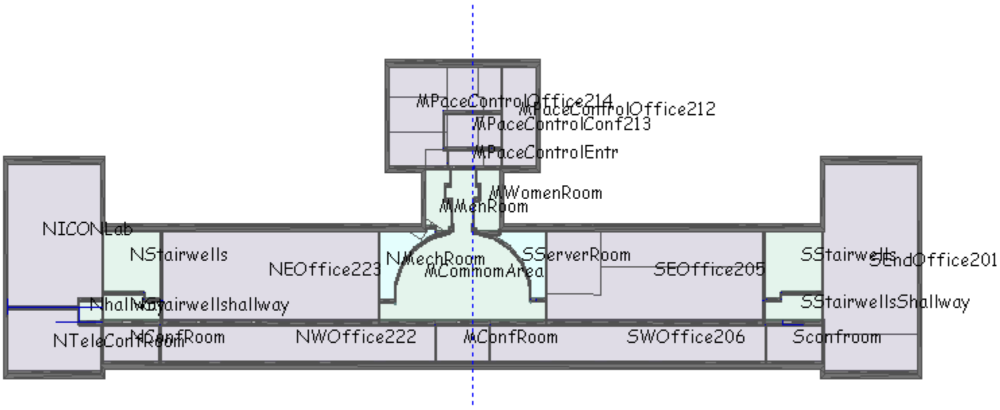


Figure 2-8 Detailed 2st floor plan

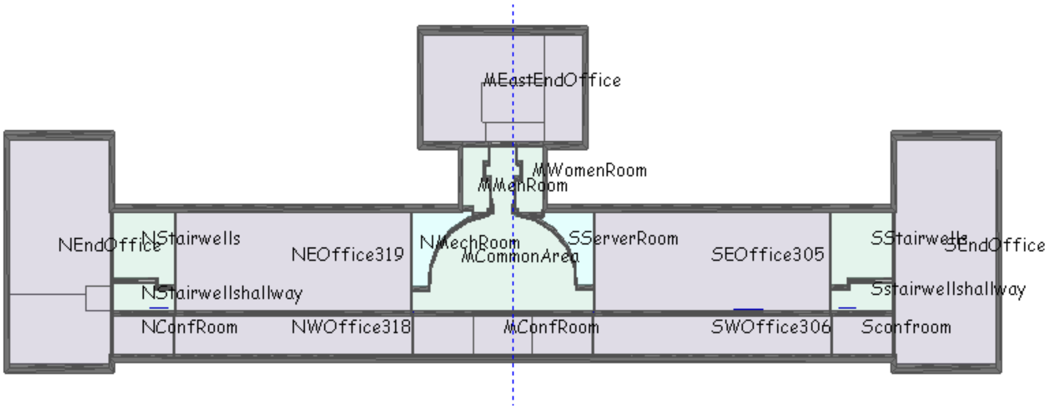


Figure 2-9 Detailed 3st floor plan

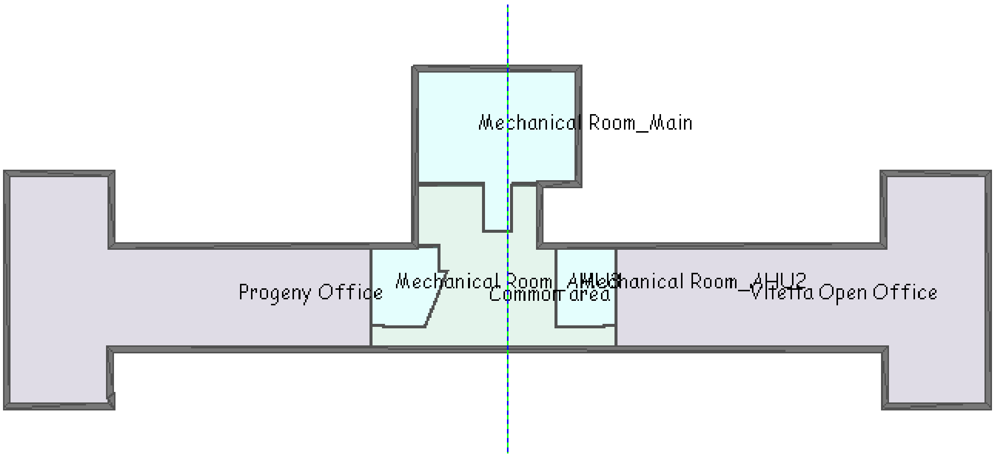


Figure 2-10 Simplified basement floor plan

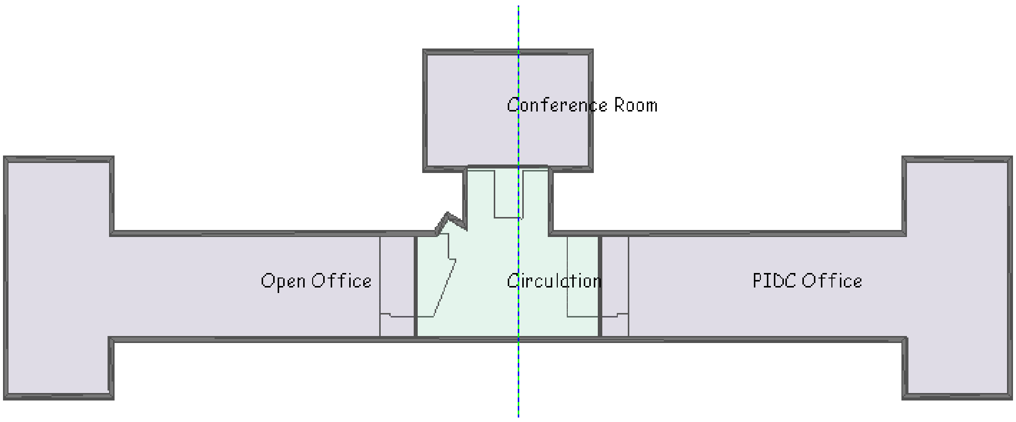


Figure 2-11 Simplified 1st floor

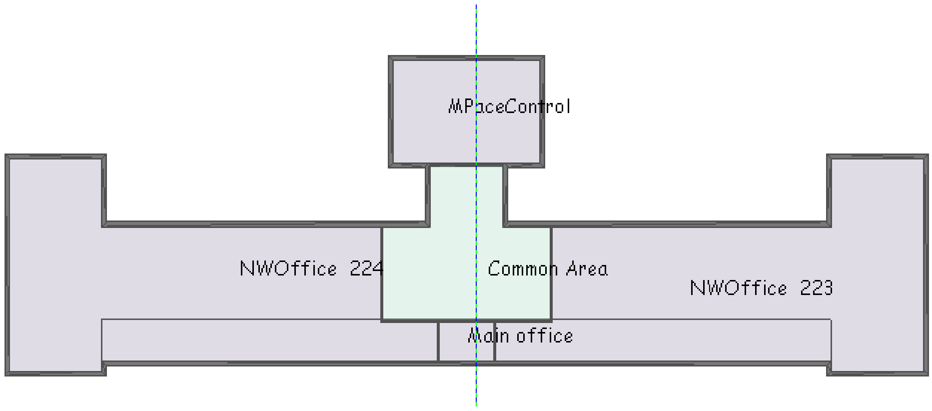


Figure 2-12 Simplified 2st floor

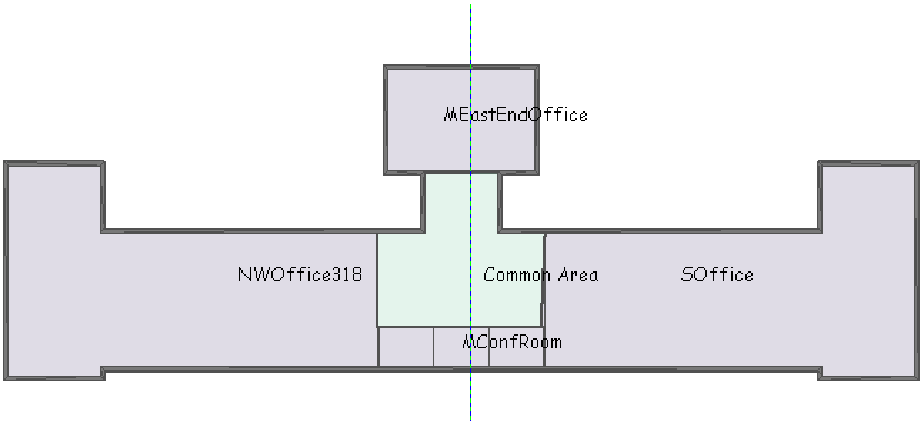


Figure 2-13 Simplified 3st floor

To generate the building energy model, the building plan and materials were modeled as specified.. For the parameter that cannot be tracked exactly, like the schedule of the office, a typical office schedule was assumed. As the building has some special control of the HVAC system, e.g. when the outside temperature is above 16 ℃, the boiler will shut down, an energy management system module was added in EnergyPlus executing this control.

In Energplus, one way of defining infiltration into each zone is through the Zone Infiltration: Design Flow Rate object and the underlying equation 2-1:

$$Infiltration = (I_{design})(F_{design})[A + B|(T_{zone-}T_{odb)}| + C(W) + D(W^2)] \qquad 2\text{-}1$$

Here the CONTAM simulation result (8760 values) are used as the $F_{design}$ and set $I_{design}$ = 1, A = 1, B = C = D = 0, so that the E+ simulation uses the CONTAM result as input.

# CHAPTER 3 CREATE A MULTI-ZONE MODEL OF BUILDING 101

## 3.1 Introduction of the process of building a multi-zone model

In this project, CONTAM is used to build the multi-zone model of the case building to calculate dynamic infiltration. To build the multi-zone model in CONTAM, one needs to zone the building reasonably to the level that it is not too complicated while not affecting the accuracy of results.

Second, one needs to calculate the wind profile coefficient of each facade. Third, one needs to estimate the ELA of each leakage component based on empirical data. In this case, the ELA of each leakage component on each facade was aggregated over the whole façade of the zone as this dramatically lightens the load of the pre-treatment of the infiltration rate results from CONTAM, especially because the case building has 394 windows in total. Fourth, one needs to get the information of the HVAC system specification.

Figures from figure 3-1 to figure 3-3 are some screenshots of the CONTAM model that was created.

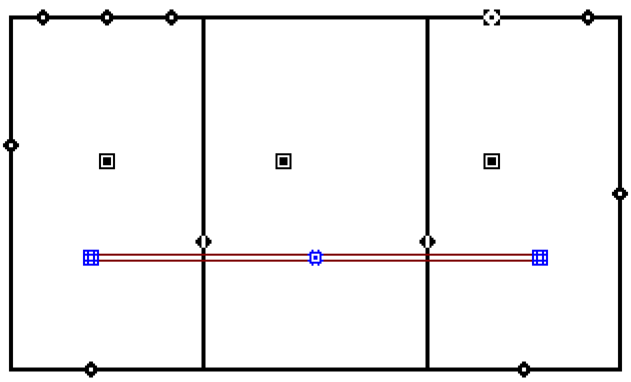

Figure 3-1 Basement floor plan in CONTAM

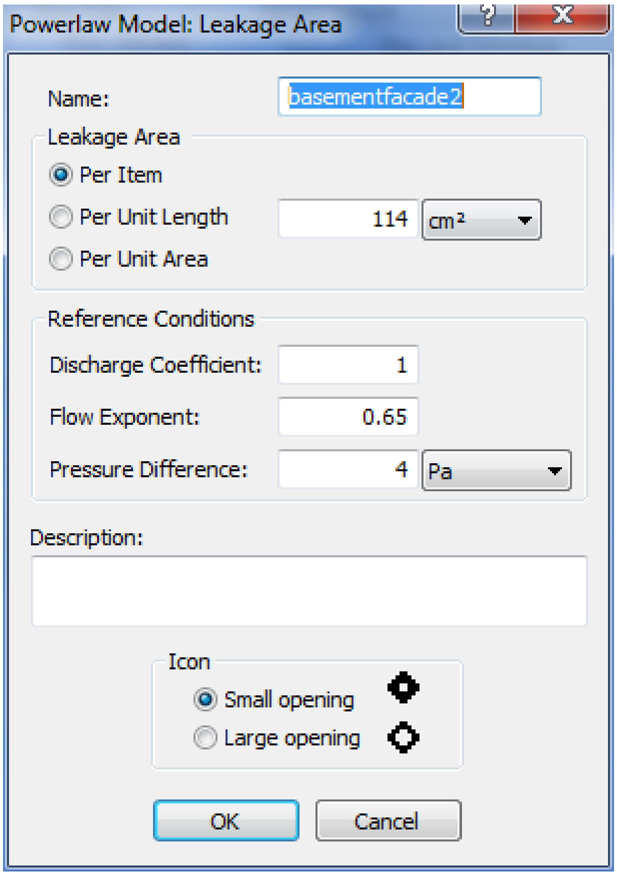


Figure 3-2 Input example of an leakage component

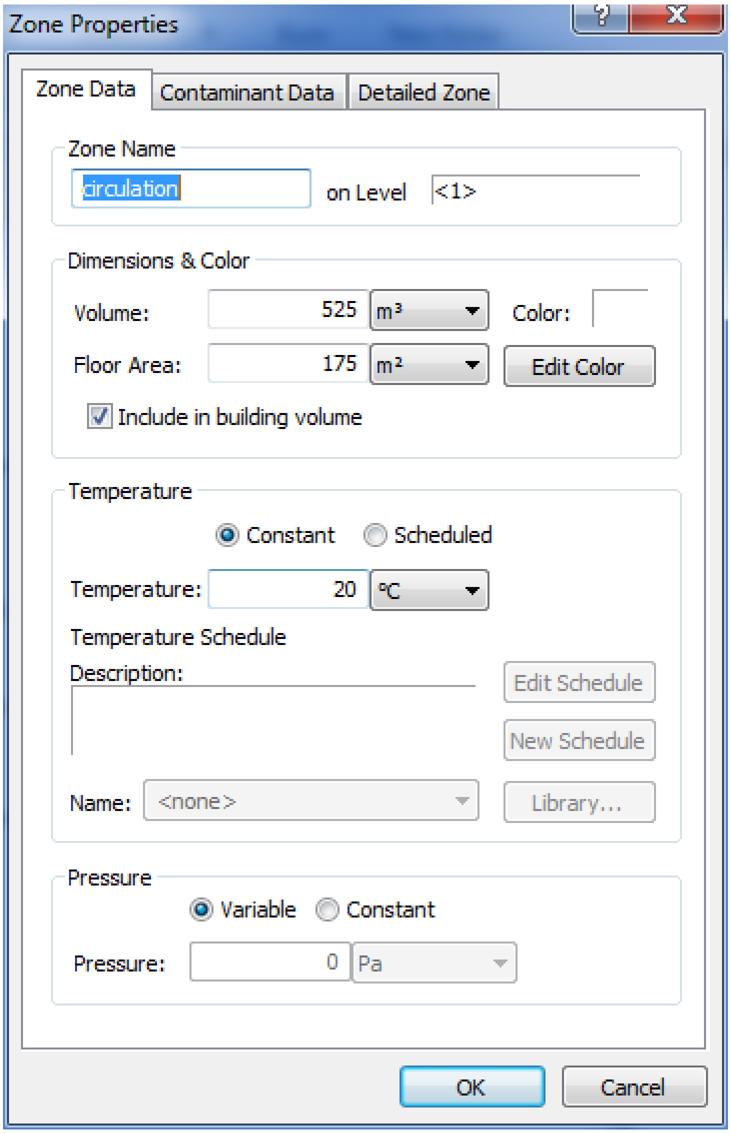


Figure 3-3 Zone information input example

## 3.2 Wind pressure coefficient calculation

To calculate the wind pressure coefficient of each facade, I utilized the web-based Cp calculator. The urban context can have a very important role of wind pressure profile calculation, from the case building's urban layout, we find this area is actually more like a suburb area, there is no building around the case building within a distance of 3 times the height of building 101. We could thus ignore the obstacle effect of surrounding buildings.

Because of model assumptions that underlie the Cp generator tool, the building shape had to simplified somewhat.

Figure 3-4 is the simplified building facade profile.

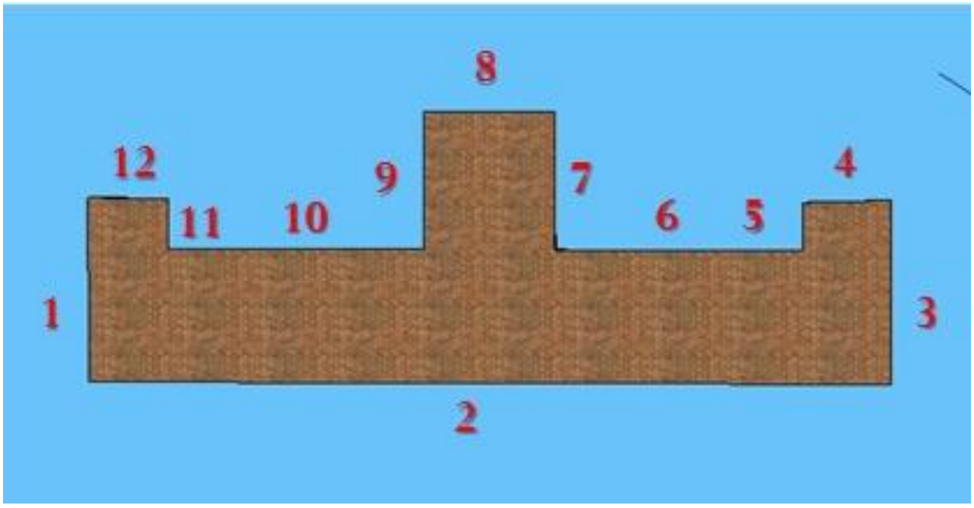


Figure 3-4 Building facade profile

In order to use the Cp generator under this facade profile, the case building was divided into 4 parts(Cp calculator can only deal with rectangular shapes). When we calculate the Cp of one part, the other three parts are considered as the obstacles around that part.

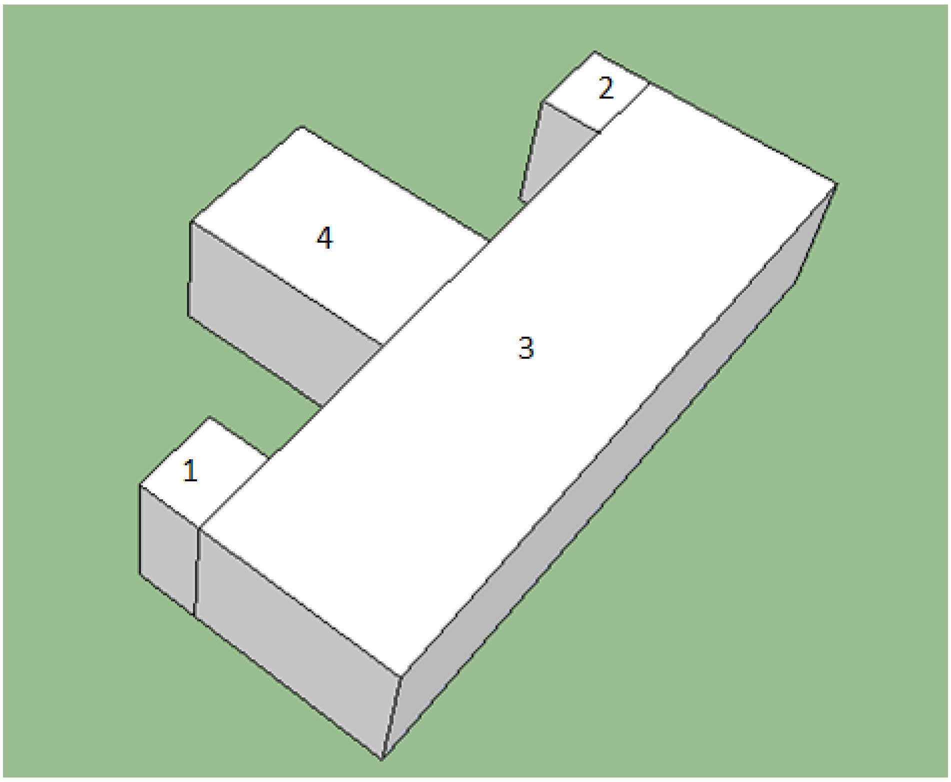


Figure 3-5 Four parts of the building

However, it was decided to not use this facade profile for the Cp calculation as the Cp calculator manual states “Too many separate obstacles close to each other, only reduce the result of the Cp prediction.” Note however that the facade profile of Figure 3-5 is used for the ELA estimates for each facade.

The actual facade profile for Cp calculation is simplified to the level shown in Figure 3-6.

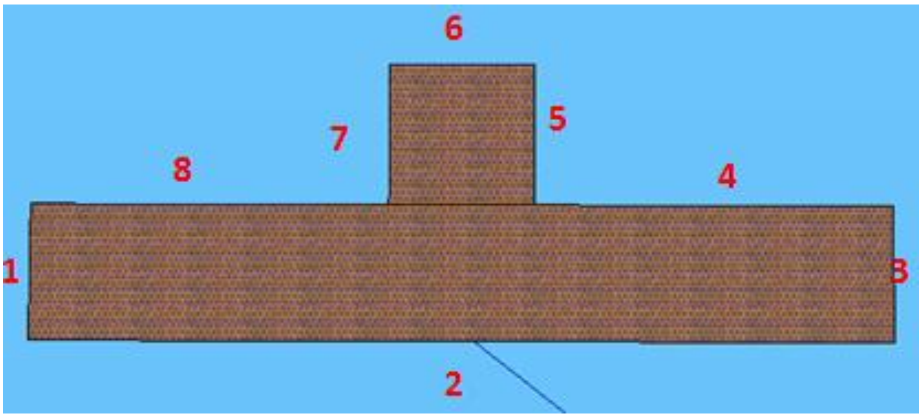


Figure 3-6 Simplified building facade profile

A text input file that contains the building information is submitted to the server to obtain the results. Below is the procedure of inputting the building information into the text file.

At the text block 'Name: building', fill in the data of the object, of which you want to have the Cp values calculated. Give coordinates X and Y for a base point of the building in your ground plan. Give the azimuth in degrees for the first facade anti-clockwise from this base point. The Length (L), Width (W) and Height (H) of the building may be followed by a key (=1) for a pitched roof, the roof angle in degrees and the size of the roof basis.

Do not adjust the name: building. Always mention this block first;

Do not adjust or remove the text block 'Name: meteo'. The default applies to meteorological wind (X or Y = 1.0E6 and H = 10). Adjust the reference wind speed by giving X, Y and H for a local meteo station. Then, the terrain roughness given at 'Wind.Zo' does also apply to the meteo station;

Change obstacle 1, obstacle 2, etc. to preferred names. Describe only major obstacles. Try and combine obstacles with built-on parts to one major obstacle. Too many separate obstacles close to each other, only reduce the result of the Cp prediction. Also define a dense wood or a hill as necessary as (block shaped) obstacles.

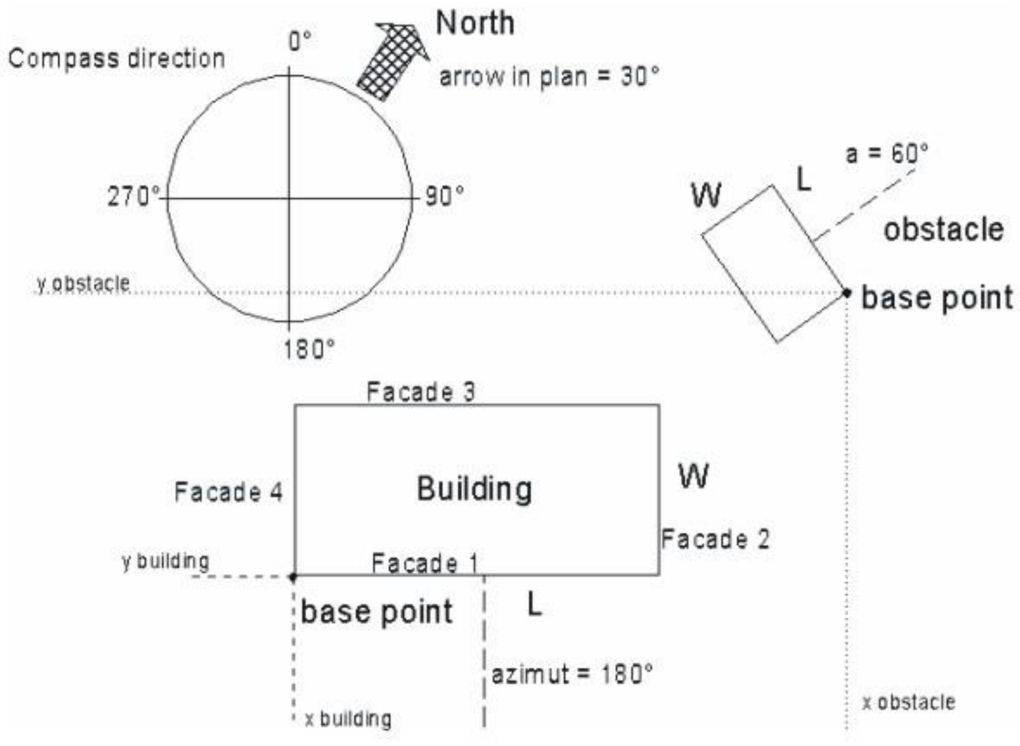


Figure 3-7 Obstacle location relative to the building

Cp-positions: Give the coordinates of the Cp points at each facade (looking towards it with X, Z = 0, 0 down left; see lower part of the figure 3-8 and the roof (looking from above with the base point situated down left is X, Y = 0, 0; see upper part of the figure 3-8. The facades are numbered anti-clockwise. The name 'Facade', followed by a space and a number (1 to 4), is mandatory. The name 'Roof' also is mandatory. The maximum number of Cp-positions = 40.

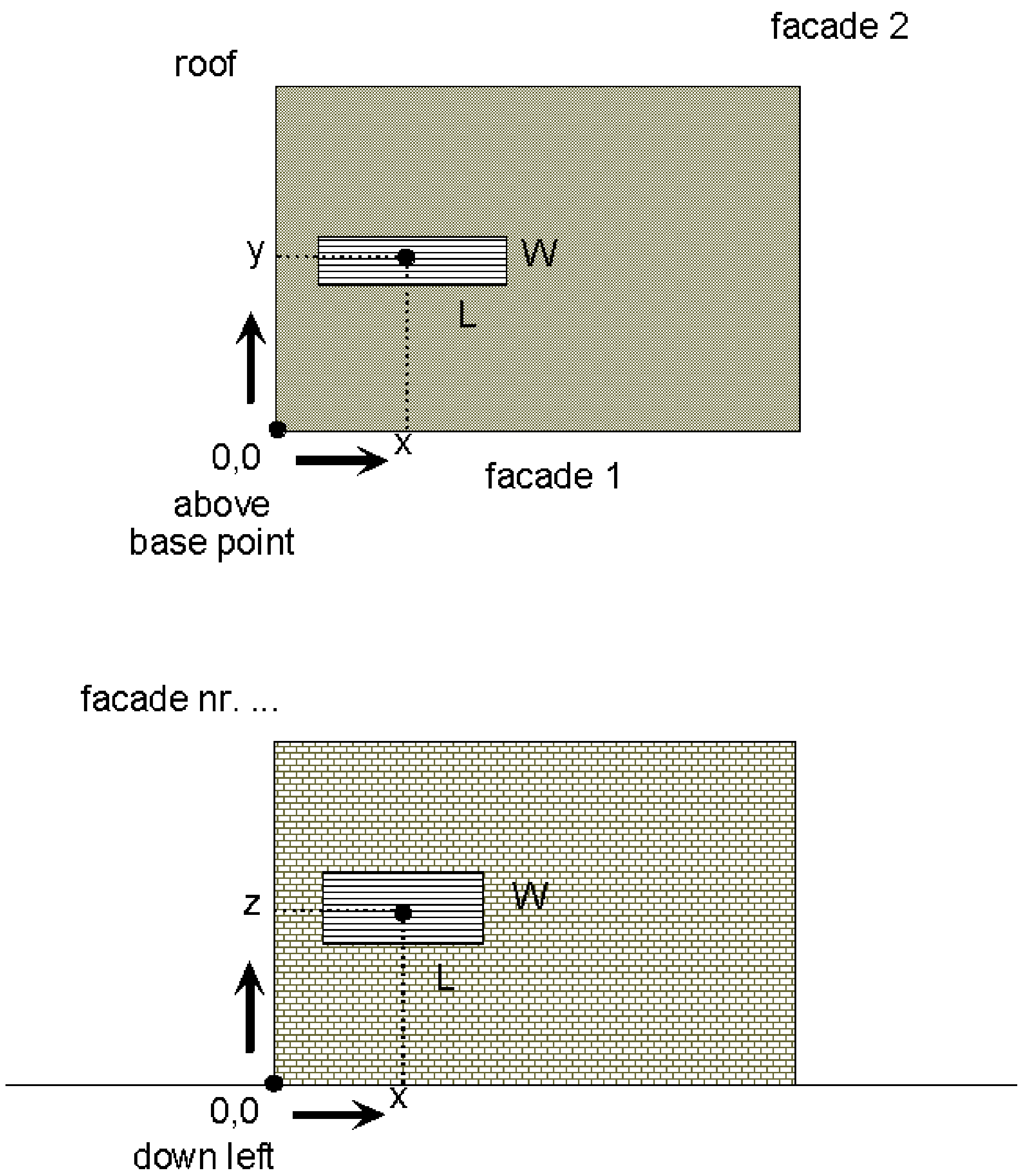


Figure 3-8 Coordinates of Cp input

The average Cp of each facade is summarized with the wind angle from o to 360 degrees.

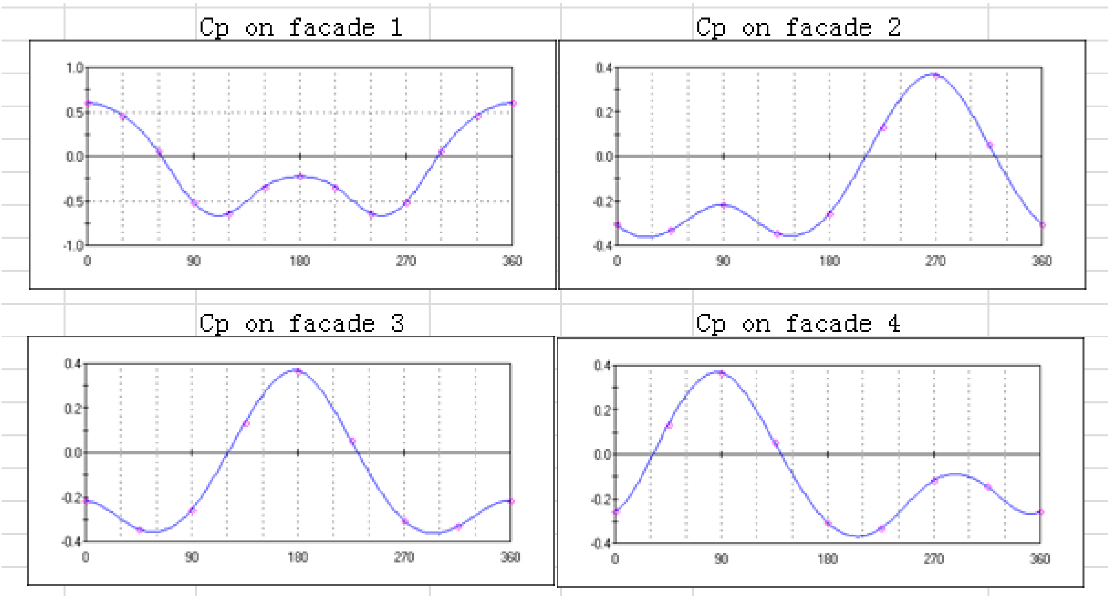


Figure 3-9 Cp value from facade 1to facade 4

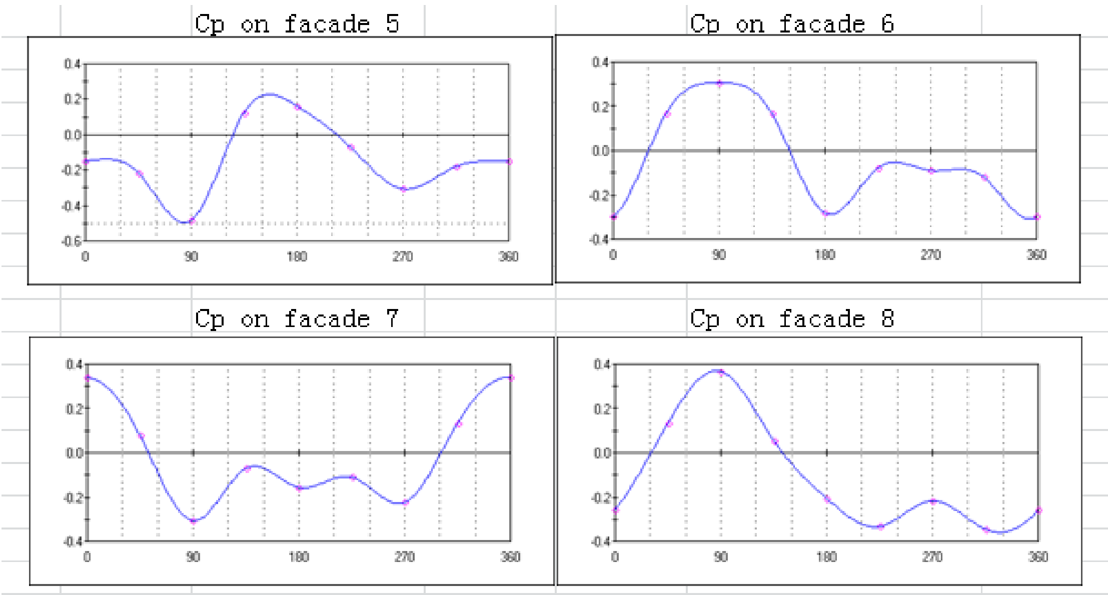


Figure 3-10 Cp value from facade 5 to facade 8

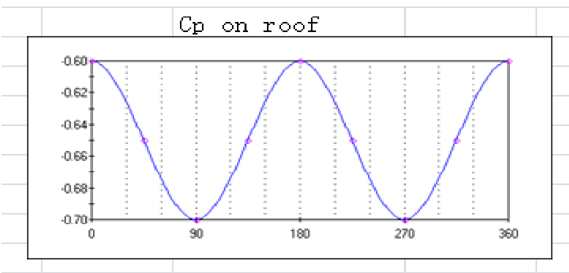


Figure 3-11 Cp value of roof

## 3.3 ELA variability estimation

Getting an estimate of ELA variability in all leakage components is an important part in the whole process. In typical building energy simulations also it is one of the most dominant sources of uncertainty. In this project, we use the window effective leakage area from Miscellaneous Commercial and Institutional Building Airtightness Data in CONTAM library to predict the ELA of the whole facade.

Table 3-1 CONTAM library data for ELA estimation

| Element Name | Building Type | Description | Model | Value | Reference |
|---|---|---|---|---|---|
| WNOO6C_CMN | Commercial | Operable window, Building C, minimum | ELA4 | 1.73 cm2/m2 | C6 |
| WNOO6C_CMX | Commercial | Operable window, Building C, maximum | ELA4 | 3.46 cm2/m2 | C6 |

For the window ELA, we average the maximum and minimum ELA, which is 2.6cm2/m2. For the roof ELA, according to the SSPC90.1 Envelope subcommittee component infiltration rate, roof leakage area is about 1/3 of window per square meter, which is 0.87cm2/m2. I assume that the percentage of ELA of each facade is 5 times of the ELA of total window. Take facade 2 in second floor as an example, the window area of facade 2 in second floor is 92m2, so the total ELA of window is 92*2.6=239.8cm2, therefore the total ELA of facade is 239.8*5= 1199cm2.

Based on the above empirical data of each leakage component, the first guess of ELA at 4pa is obtained.

Table 3-2 First guess of ELA at 4Pa (Total ELA=10905cm2)

| Basement | ELA(cm2) | First floor | ELA(cm2) | Second floor | ELA(cm2) | Third floor | ELA(cm2) |
|---|---|---|---|---|---|---|---|
| Facade1 | 135 | Facade1 | 339 | Facade1 | 189 | Facade1 | 189 |
| Facade2 | 77 | Facade2 | 1122 | Facade2 | 1220 | Facade2 | 695 |
| Facade3 | 135 | Facade3 | 339 | Facade3 | 189 | Facade3 | 189 |
| Facade4 | 38 | Facade4 | 97 | Facade4 | 54 | Facade4 | 54 |
| Facade5 | 19 | Facade5 | 97 | Facade5 | 0 | Facade5 | 54 |
| Facade6 | 173 | Facade6 | 679 | Facade6 | 215 | Facade6 | 215 |
| Facade7 | 19 | Facade7 | 339 | Facade7 | 189 | Facade7 | 108 |
| Facade8 | 77 | Facade8 | 194 | Facade8 | 108 | Facade8 | 108 |
| Facade9 | 19 | Facade9 | 194 | Facade9 | 189 | Facade9 | 108 |
| Facade10 | 96 | Facade10 | 533 | Facade10 | 215 | Facade10 | 215 |
| Facade11 | 19 | Facade11 | 97 | Facade11 | 54 | Facade11 | 108 |
| Facade12 | 38 | Facade12 | 97 | Facade12 | 0 | Facade12 | 54 |
| Roof | 1199 | | | | | | |

With this first guess of ELA values (aggregated per zone in the energy model), the energy simulation was performed and outcomes of the boiler gas consumption from the energy model are compared with the monitored data. The result is shown below:

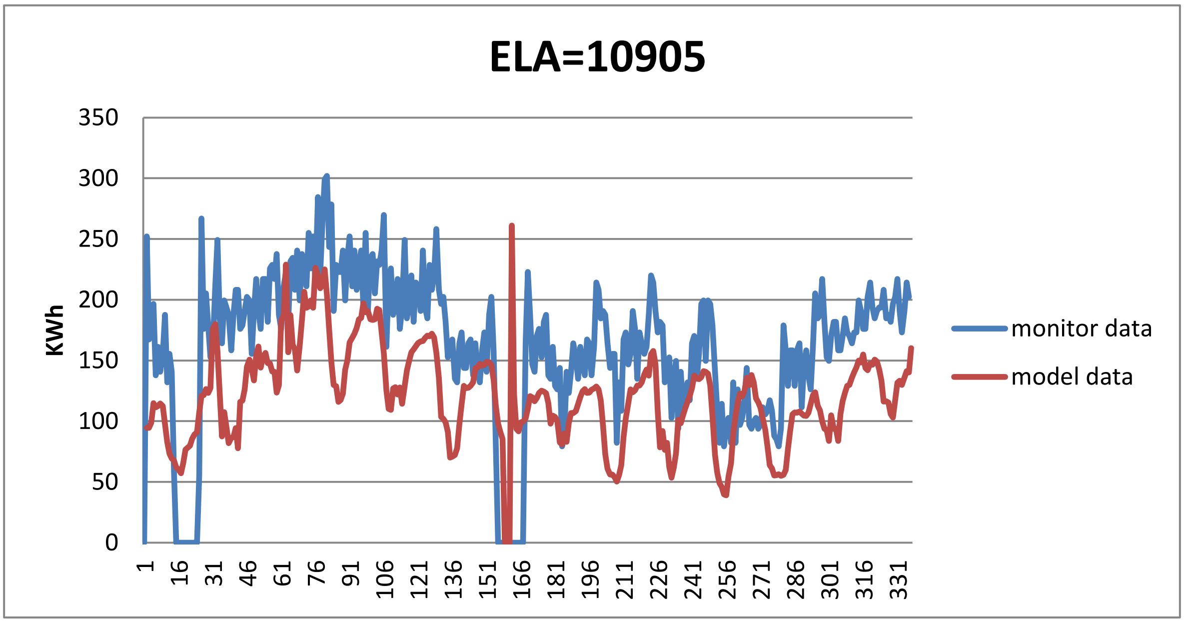


Figure 3-12 Boiler gas consumption with ELA=10905cm2

This boiler gas consumption is two weeks data from JAN/01 to JAN/14 2012, from the graph, an eyeball examination shows that the energy model consumption is consistently smaller than the monitor data on average, therefore, after this first simulation,  the next ELA estimate should be bigger than our first guess of 10905.. Also, we notice that during two periods, one from the beginning, the other in the middle, the boiler is actually turned off. However, according to  the specification, there is no heating setback during the weekend, the boiler will be turned off only if it senses the outside temperature to be higher than 16℃. This occurs only once as can be seen from the red line around hour 160. It has to be assumed that there must have been  manual intervention to turn the boiler off, or in the real condition, the outside temperature the sensor sensed is different from the weather data we obtained for the measurement period. To make things comparable, it was decided to delete the period when the monitor boiler consumption is 0. Here is the refined result:

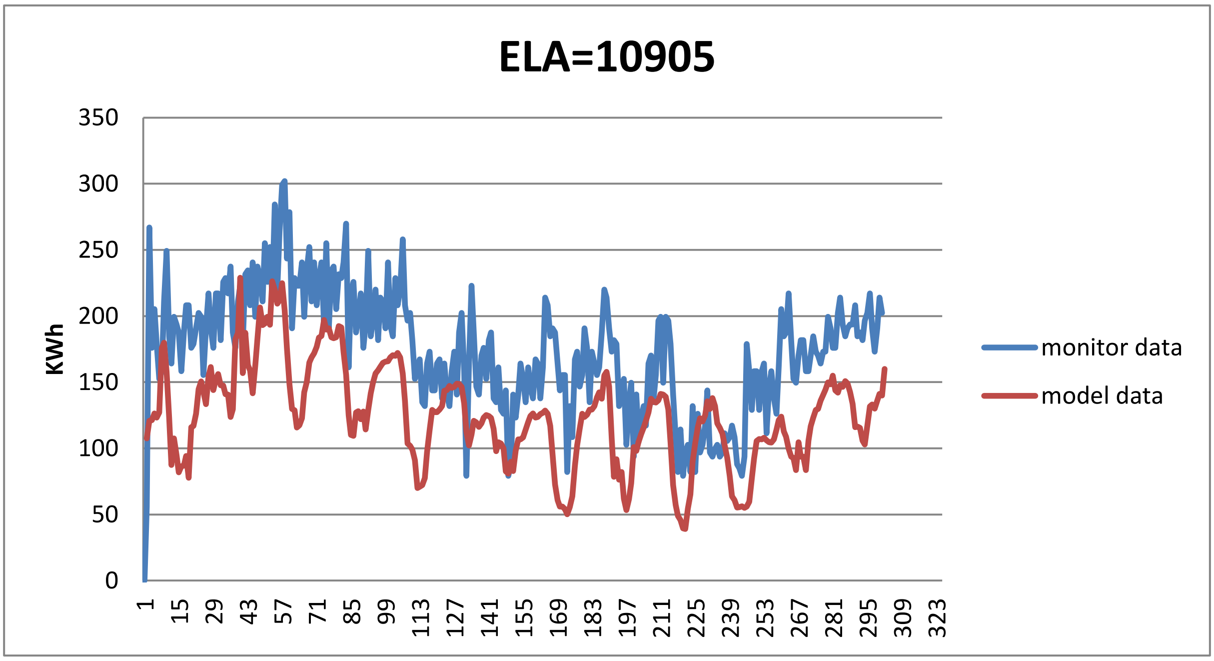


Figure 3-13 Boiler gas consumption without weekend

The following ELA estimations are basically generated proportional to the ELA=10905cm2 at 4 pa. Not all  ELA samples are listed in this chapter; only the best estimate of the ELA is listed in table 3-3, where the total building ELA is 23437cm2 at 4 Pa. Other results are contained in the Appendix. The ELA estimate of each facade here is 2.15 times compared to the case where the total building ELA=10905cm2.

Table 3-3 Total ELA=23437cm2

| Basement | ELA(cm2) | First floor | ELA(cm2) | Second floor | ELA(cm2) | Third floor | ELA(cm2) |
|---|---|---|---|---|---|---|---|
| Facade1 | 290 | Facade1 | 730 | Facade1 | 406 | Facade1 | 406 |
| Facade2 | 166 | Facade2 | 2415 | Facade2 | 2626 | Facade2 | 1496 |
| Facade3 | 290 | Facade3 | 730 | Facade3 | 406 | Facade3 | 406 |
| Facade4 | 83 | Facade4 | 209 | Facade4 | 116 | Facade4 | 116 |
| Facade5 | 41 | Facade5 | 209 | Facade5 | 0 | Facade5 | 116 |
| Facade6 | 373 | Facade6 | 1461 | Facade6 | 464 | Facade6 | 464 |
| Facade7 | 41 | Facade7 | 730 | Facade7 | 406 | Facade7 | 232 |
| Facade8 | 166 | Facade8 | 417 | Facade8 | 232 | Facade8 | 232 |
| Facade9 | 41 | Facade9 | 417 | Facade9 | 406 | Facade9 | 232 |
| Facade10 | 207 | Facade10 | 1148 | Facade10 | 464 | Facade10 | 464 |
| Facade11 | 41 | Facade11 | 209 | Facade11 | 116 | Facade11 | 232 |
| Facade12 | 83 | Facade12 | 209 | Facade12 | 0 | Facade12 | 116 |
| roof | 2580 | | | | | | |

The comparison result from the best ELA estimate is shown in Figure 3-14 below:

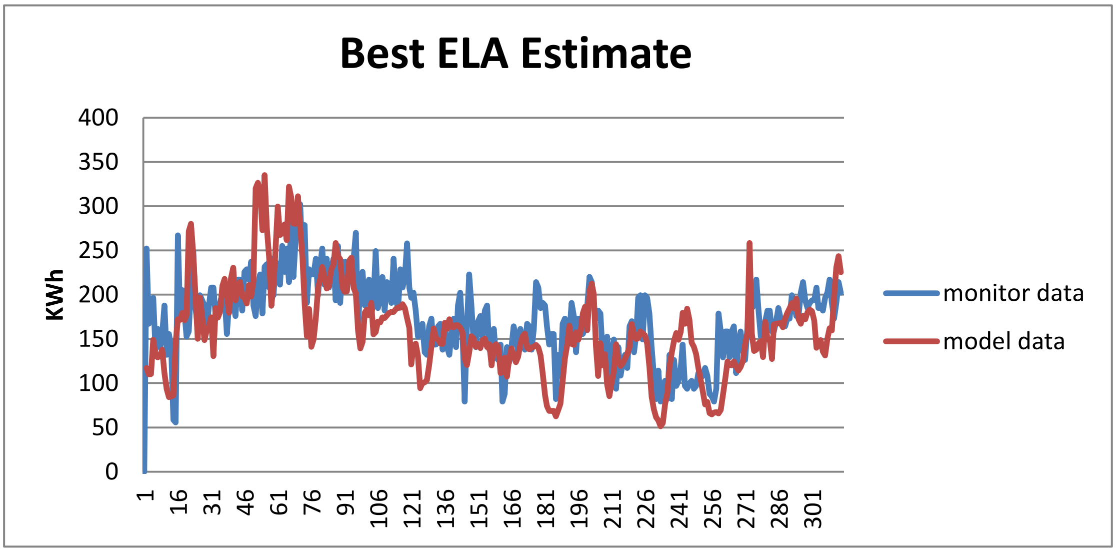


Figure 3-14 Boiler gas consumption with best ELA estimate

## 3.4 Method to determine which ELA is the best estimate

The indicator used to determine which ELA is the best estimation is Mean Square Error (MSE). In statistics, the mean squared error (MSE) of an estimator is one of many ways to quantify the difference between values implied by an estimator and the true values of the quantity being estimated. MSE is a risk function, corresponding to the expected value of the squared error loss or quadratic loss. MSE measures the average of the squares of the "errors." The error is the amount by which the value implied by the estimator differs from the quantity to be estimated. The formula of MSE is as equation 3-1:

$$MSE = \frac{1}{n}\sum_{i=1}^{n}\left(\widehat{Y_i} - Y_i\right)^2 \qquad 3\text{-}1$$

$\hat{Y}$ is a vector of n predictions

$Y$ is the vector of the true values

In this particular case, $Y$ is the real monitor data of boiler gas consumption, $\hat{Y}$ is the predicted data from the EnergyPlus model.

# CHAPTER 4 CONCLUSION AND RECOMMENDATION

## 4.1 Conclusion from the current result:

Table 4-1 Blower door test result

| Table 2. Analysis Results Whole Building Depressurization Test. | |
|---|---|
| Air leakage at 50 Pascals | 27,990 cfm |
| Air leakage at 75 Pascals | 36,112 cfm |
| 95% confidence interval | 0.7 % |
| Correlation coefficient squared ($R^2$) | 0.999 |
| Flow exponent (n) | 0.628 |
| Air leakage coefficient (C) | 2,396.0 cfm/$Pa^n$ |
| Equivalent leakage area @ 10 Pa | 2,991.4 sq. in. |
| Effective leakage area @ 4 Pascals | 1,624.8 sq. in. |
| Whole building enclosure area | 87,200 ft2 |
| Building Volume | 948,297 ft3 |
| Cfm75/ft2 enclosure (all six sides) | 0.41 |
| $ACH_{50}$ | 1.8 |

Based on the whole building depressurization test, we can see that the power law of the whole building is Q= 2396*$(\Delta p)^{0.628}$, based on this equation, we can calculate the air leakage rate of the whole building is 2.7 m3/s, 0.36 ACH at 4 Pa, ELA is 10483cm2 at 4Pa.

As shown in the last chapter, the best estimation of ELA at 4Pa is 23437cm2, while the ELA estimate from the blower door test being 10483 cm2 at 4Pa. However, because of the uncertainty of the energy model and multi-zone model, this result is not a conclusive adoption or rejection of the new inverse approach as predictor of the ELA of the building. There are some reasons that uncertainty could explain the discrepancy. Firstly, the energy model contains many sources of uncertainty. Although the input of the energy model is based on the building specification, there could still be big discrepancies between the modeled and real usage and operation scenario, especially relevant to the HVAC system modeling. In fact, to simplify the HVAC modeling, a compact VAV system was used with auto sizing instead of a detailed HVAC system and specific nameplate capacity of the equipment (which was not available in the specification)

Secondly, the biggest uncertainty resource of modeling the multi-zone model is the airflow control part of the HVAC system modeling. As the system in the case building is a VAV system, as it is hard to predict the dynamic airflow rate of the air outlet and thereby any variations in room pressure resulting from the HVAC operation. Currently, a simple schedule based on the fresh air schedule to the airflow fans is assumed. As a result, the set-pressure of each outlet could be at times bigger than in the real case, which would result in a reduction of the infiltration rate at a certain ELA., As a consequence the ELA predicted by the inverse modeling process will be higher than the blower door test would indicate.

## 4.2 Simple uncertainty analysis

The following rudimentary uncertainty analysis is about estimating the probable ELA distribution as a result of the uncertainty of the CONTAM model. for this purpose we assume that the actual infiltration rate is with the range of 0.8V to 1.2 V, where V is the deterministic result from the CONTAM model. Then, based on this ±20% infiltration range, we can find the ELA estimate range that could result from this variation, thus get the uncertainty distribution of the ELA as a result of CONTAM modeling error. As shown above, the best estimate of the ELA is 23437cm2, with infiltration rate equals 2.25m3/s for the whole building. Below is the infiltration rate range from a baseline calculated with ELA =23437cm2 at 4 Pa.

Table 4-2 Infiltration rate range from the baseline ELA=23437cm2

| | |
|---|---|
| ELA | 23437cm2 |
| Average infiltration rate(m3/s) | 2.25 |
| Average ACH | 0.3 |
| Base infiltration rate(m3/s) | 2.25 |
| -20% | 1.80 |
| 20% | 2.70 |

Therefore, the ELA values that result in infiltration values between 1.8m3/s and

2.7m3/s is the range of possible ELA values. Through calculation, the best match of the ELA that result in 1.8cm3/s and 2.7m3/s is 18240cm2 and 29403cm2 respectively.

Table 4-3 ELA margin under CONTAM model uncertainty

| | |
|---|---|
| Infiltration rate from ELA=23437cm2(m3/s) | 2.25(0%) |
| Infiltration rate from ELA=18240cm2(m3/s) | 1.8(-20%) |
| Infiltration rate from ELA=29403cm2(m3/s) | 2.7(+20%) |

From this calculation, we could say with our assumption that uncertainty to calculate the infiltration rate is ±20% under CONTAM model uncertainty, the ELA could lie between (18240cm2, 29403cm2), as shown in figure4-1, which shows the possible ELA distribution as a result of CONTAM modeling uncertainty. Although the ELA value 10483cm2 from the blower door test does not lie in this range, that may because we only consider the uncertain of the CONTAM model, with other parameters uncertainty taken into account, the ELA=10483cm2 could be within the range.

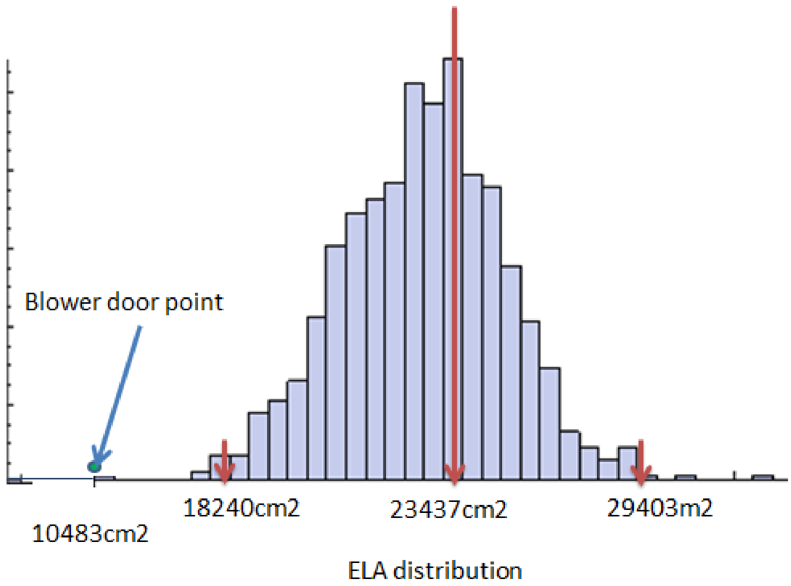


Figure 4-1 ELA distribution as a result of CONTAM modeling uncertainty

Figure 4-2 show the qualitative outcome of an extended uncertainty analysis, where we add multiple sources of uncertainty. Such a study is intended as a follow up, and will be used to determine the confidence that the ELA estimate is within a given range. Based on the initial outcome above for a reasonable assumption of the uncertainty in the CONTAM model, it is likely that this range will be too large to give confidence intervals that are good enough to rely on the method proposed in this thesis.

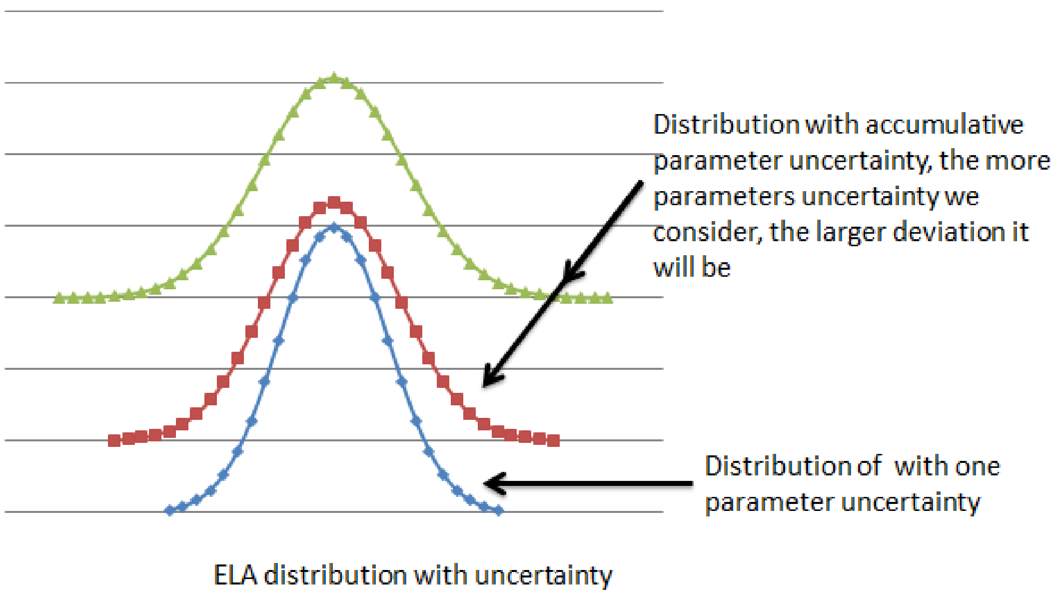


Figure 4-2 ELA distribution (qualitative) with multiple parameters uncertainty

Until now we have only considered the calibration of one parameter. In case we do multi parameter calibration (as shown in figure 4-3 for schedule and building material parameters) we may get better calibration results for ELA. At this point in time this expectation is purely speculative. At the very least it can be expected that more detailed monitor data (not just hourly energy consumption) should be available to make this work.

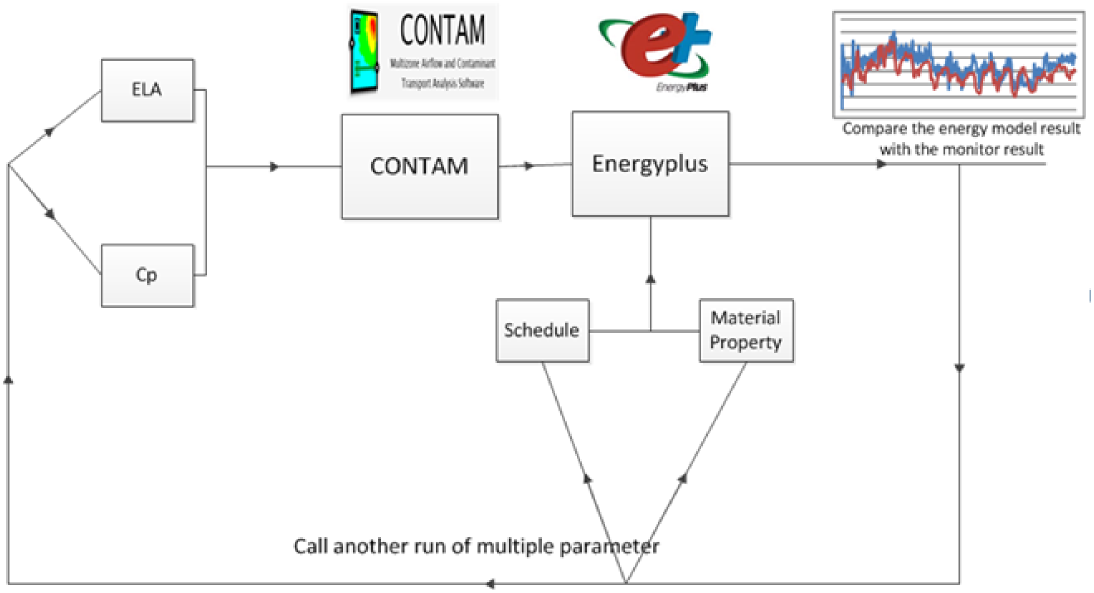


Figure 4-3 Multi-variable analysis diagram

# CHAPTER 5 FUTURE WORK

## 5.1 Automation of the calibration process

There are a lot of manually work during the whole process, which could be avoided if we accomplish succeed to connect the CONTAM and EnergyPlus and let them run automatically. If we can accomplish this automation process, we can conduct a full optimization process even with multiple variables or propagate multiple parameter uncertainties to get a more reliable result.

The good news is our research group is developing an EnergyPlus wrapper in the Model-Center tool (Phoenix model center website). With addition of a CONTAM wrapper, full automation will be accomplished. With the help of model center, the efficiency of the simulation will be dramatically improved.

As an alternative of the CONTAM, the nodal airflow network in the EnergyPlus could also be employed as a multi-zone model to calculate the dynamic infiltration rate. The reason why this module is not used in this practice is because there are so many leakage components of the case building, that if we want to employ this module, we need to define each leakage component one-by-one which is time consuming, while in the CONTAM mode, one can just aggregate the leakage component of each facade together as one big leakage component. Another reason is that current nodal airflow network can only deal with the constant volume HVAC system.

Actually, the first problem can be solved through simplifying the energy model, for example, we can aggregate all the windows in one facade into a aggregated window to represent them, it will not affect the energy simulation results a lot but will dramatically simplify the input procedure.

For the HVAC system modeling problem, the VAV system is a difficult part to model, since it is hard to estimate the dynamic airflow rate from the airflow outlet. Even if one chooses a reasonable schedule for the air outlet in the CONTAM model, there still could be a big deviation from the real operation condition.

With the embedded nodal airflow network we can more easily accomplish the automation process since now we only need the EnergyPlus wrapper in model center. Therefore with more developments added to the nodal airflow network module in EnergyPlus, we will no longer need CONTAM to simulate dynamic infiltration in the future.

## 5.2 Calibration under uncertainty

There are still a lot of uncertainties of different parameters like the Cp of each facade, material properties, etc. Therefore, it is more convincing to do the same procedure under uncertainty.

There are basically three different levels to do the uncertainty analysis.

First level is to create an ELA band to see how many hours the hourly monitor data will lie in the output from the energy model, then we can calculate the confidence that the ELA is within this band. Definitely this approach is rough and unreliable, but this is the easiest way to assess the role of uncertainty.

The second one is that we can do the prior uncertainty quantification for dominant parameters, for example, material properties, and COP of the HVAC system, based on the empirical data from expert judgment, which could be derived from a pool of sources (experiments, surveys, expert knowledge, industry standards, etc). After we got the distribution of these parameters, we can run the Monte Carlo simulation with the distribution of these parameters and get a distribution of the ELA estimate. For each run, the indicator of the best estimate is the Mean Square Error (MSE) of monitor data and model data. Figure 5-1 is a system diagram of this approach.

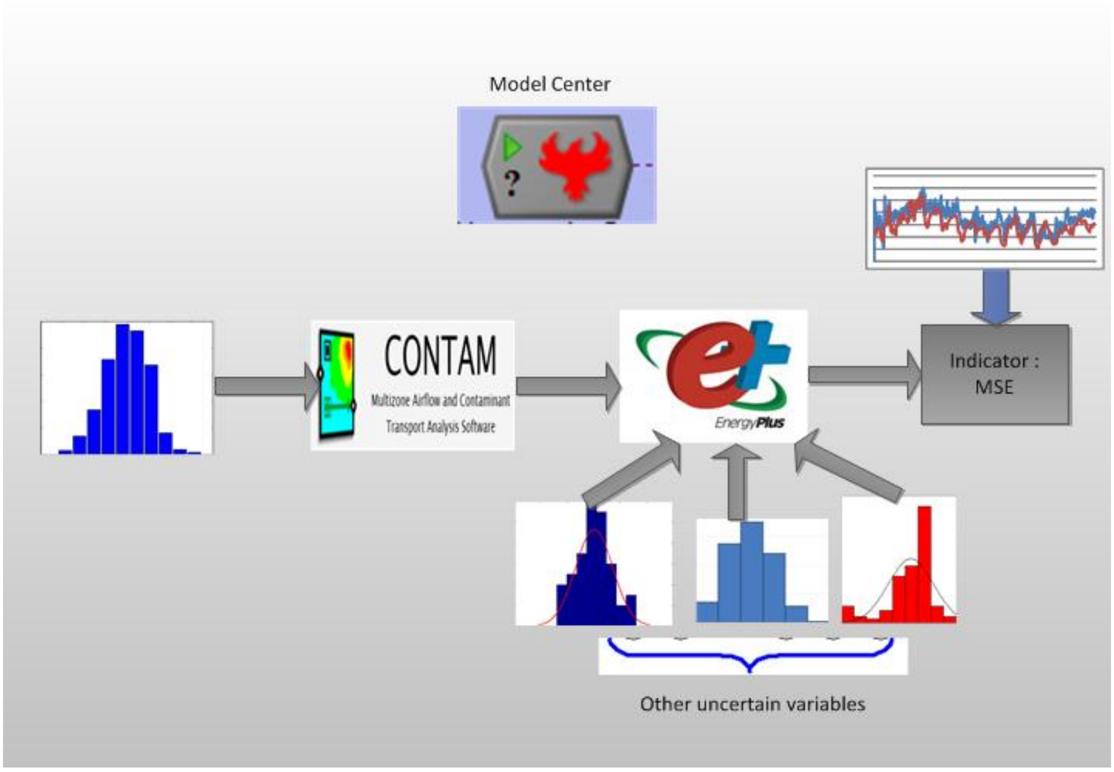


Figure 5-1 Uncertainty analysis execution

The third one is the most difficult one, using a high-level mathematical Bayesian calibration method [8].

The mathematical formulation of Bayesian calibration is developed by Kennedy and O'Hagan [9]. The statistical formula captures three types of uncertainties: (a) parameter uncertainty in the energy simulation model, (b) discrepancy between the model and the true behavior of the building, and (c) observation errors. We quantify these uncertainties with respect to known conditions x under which the observations are taken. The relationship between observations and model outputs follows:

$$y(x)=\eta(x) + \delta(x) + \varepsilon(x)$$

Observations are denoted by y(x); $\eta(x, \theta)$ denotes building energy model outputs computed at known conditions x (e.g. external temperature, known schedule, etc.) and calibration parameters θ. Since the energy model is based on approximation of all physical and occupant processes occurring in a building it will not represent the actual true consumption of the building. This discrepancy between the model and the true physical behavior of the building is represented by $\delta(x)$. This term prevents over-estimation of calibration values, and describes how the energy model falls short. Any errors in recording observations (energy consumption in this case) are denoted by $\varepsilon(x)$.

In the Bayesian paradigm uncertain parameters are assigned prior distributions $p(\theta)$ the same as in the second approach above. However, the prior distributions are updated using observations through a formal set up in which the likelihood of obtaining observations from the building energy model derives the updating process through a Gaussian process. As a result, we collect plausible distributions of calibration parameters , also known as posterior distributions.

For multi-parameters calibration analysis, it is very important to do sensitivity analysis first to rank parameters by their relative effect on the energy consumption of the building. In her paper, Heo used the Morris method to do the sensitivity analysis, which is executed with the software Simlab version 2.2.

Future work should attempt all of the above methods in consecutive steps of increasing complexity and effort, ultimately leading to reliable results and confidence intervals on the range of the ELA in comparison to the ELA determined from physical experimentation with the blower door. The results of these studies will reveal whether the hypothesis that the blower door test can be replaced can be confirmed.

# APPENDIX A ELA LISTS AND COMPARISON RESULTS

1. Total ELA=10905cm2 at 4pa

| Basement | ELA(cm2) | First floor | ELA(cm2) | Second floor | ELA(cm2) | Third floor | ELA(cm2) |
|---|---|---|---|---|---|---|---|
| Facade1 | 135 | Facade1 | 339 | Facade1 | 189 | Facade1 | 189 |
| Facade2 | 77 | Facade2 | 1122 | Facade2 | 1220 | Facade2 | 695 |
| Facade3 | 135 | Facade3 | 339 | Facade3 | 189 | Facade3 | 189 |
| Facade4 | 38 | Facade4 | 97 | Facade4 | 54 | Facade4 | 54 |
| Facade5 | 19 | Facade5 | 97 | Facade5 | 0 | Facade5 | 54 |
| Facade6 | 173 | Facade6 | 679 | Facade6 | 215 | Facade6 | 215 |
| Facade7 | 19 | Facade7 | 339 | Facade7 | 189 | Facade7 | 108 |
| Facade8 | 77 | Facade8 | 194 | Facade8 | 108 | Facade8 | 108 |
| Facade9 | 19 | Facade9 | 194 | Facade9 | 189 | Facade9 | 108 |
| Facade10 | 96 | Facade10 | 533 | Facade10 | 215 | Facade10 | 215 |
| Facade11 | 19 | Facade11 | 97 | Facade11 | 54 | Facade11 | 108 |
| Facade12 | 38 | Facade12 | 97 | Facade12 | 0 | Facade12 | 54 |
| Roof | 1199 | | | | | | |

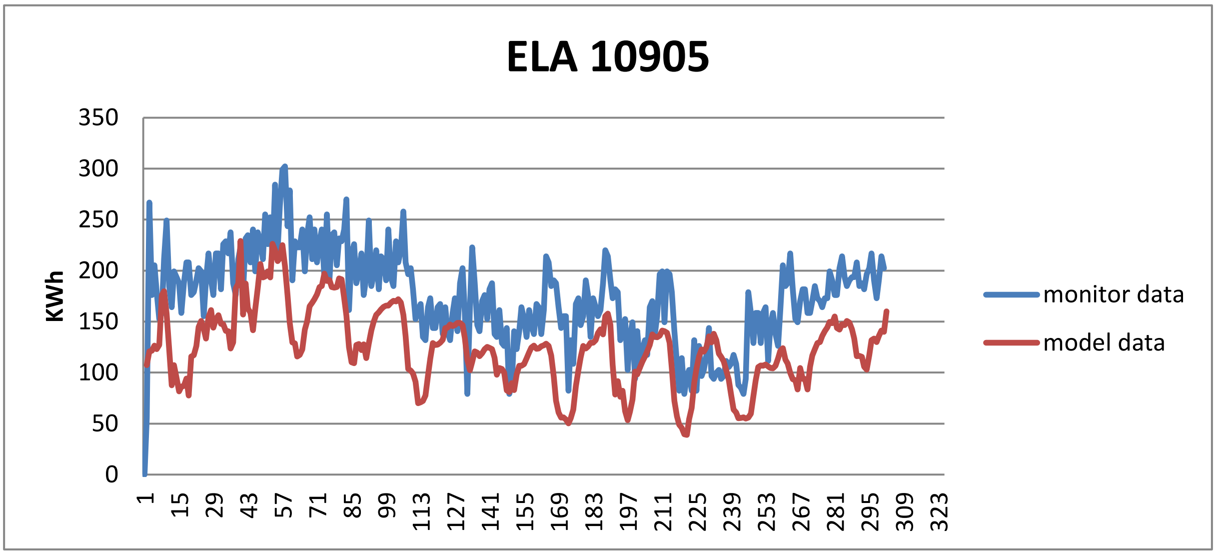


$\sqrt{MES}$=56

2. Total ELA=16172cm2at4pa

| Basement | ELA(cm2) | First floor | ELA(cm2) | Second floor | ELA(cm2) | Third floor | ELA(cm2) |
|---|---|---|---|---|---|---|---|
| Facade1 | 200 | Facade1 | 504 | Facade1 | 280 | Facade1 | 280 |
| Facade2 | 114 | Facade2 | 1666.4 | Facade2 | 1812 | Facade2 | 1032 |
| Facade3 | 200 | Facade3 | 504 | Facade3 | 280 | Facade3 | 280 |
| Facade4 | 57 | Facade4 | 144 | Facade4 | 80 | Facade4 | 80 |
| Facade5 | 29 | Facade5 | 144 | Facade5 | 0 | Facade5 | 80 |

| | | | | | | | |
|---|---|---|---|---|---|---|---|
| Facade6 | 257 | Facade6 | 1008 | Facade6 | 320 | Facade6 | 320 |
| Facade7 | 29 | Facade7 | 504 | Facade7 | 280 | Facade7 | 160 |
| Facade8 | 114 | Facade8 | 288 | Facade8 | 160 | Facade8 | 160 |
| Facade9 | 29 | Facade9 | 288 | Facade9 | 280 | Facade9 | 160 |
| Facade10 | 143 | Facade10 | 792 | Facade10 | 320 | Facade10 | 320 |
| Facade11 | 29 | Facade11 | 144 | Facade11 | 80 | Facade11 | 160 |
| Facade12 | 57 | Facade12 | 144 | Facade12 | 0 | Facade12 | 80 |
| Roof | 1780 | | | | | | |

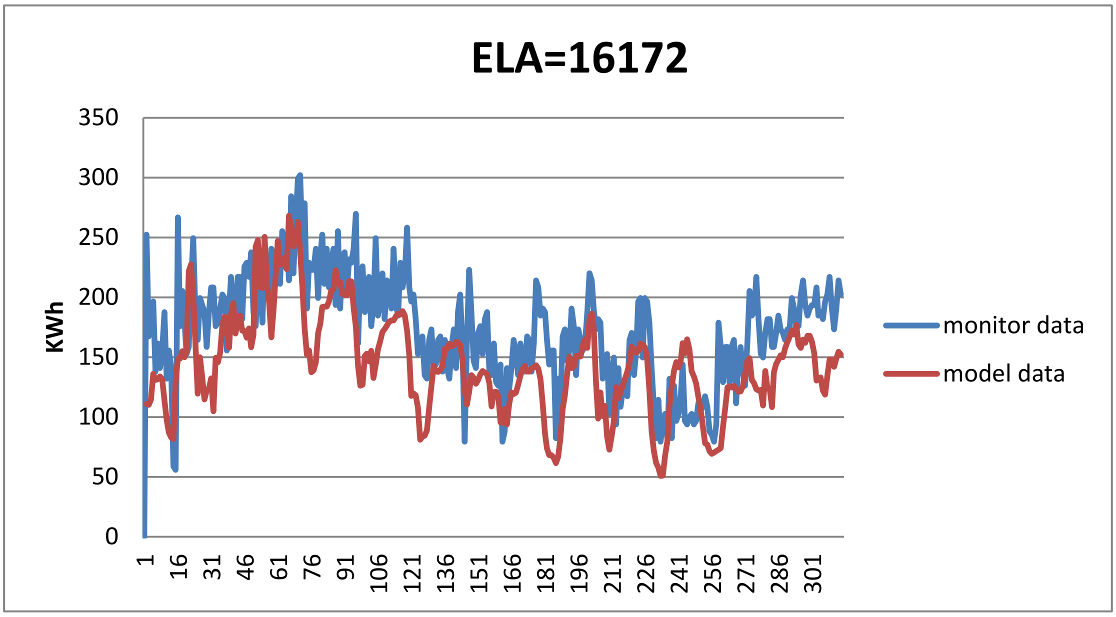


$\sqrt{MES}$=42.9

3. Total ELA=18717cm2at4pa

| Basement | ELA(cm2) | First floor | ELA(cm2) | Second floor | ELA(cm2) | Third floor | ELA(cm2) |
|---|---|---|---|---|---|---|---|
| Facade1 | 231 | Facade1 | 583 | Facade1 | 324 | Facade1 | 324 |
| Facade2 | 132 | Facade2 | 1926 | Facade2 | 2095 | Facade2 | 1193 |
| Facade3 | 231 | Facade3 | 583 | Facade3 | 324 | Facade3 | 324 |
| Facade4 | 66 | Facade4 | 166 | Facade4 | 92 | Facade4 | 92 |
| Facade5 | 33 | Facade5 | 166 | Facade5 | 0 | Facade5 | 92 |
| Facade6 | 297 | Facade6 | 1165 | Facade6 | 370 | Facade6 | 370 |
| Facade7 | 33 | Facade7 | 583 | Facade7 | 324 | Facade7 | 185 |
| Facade8 | 132 | Facade8 | 333 | Facade8 | 185 | Facade8 | 185 |
| Facade9 | 33 | Facade9 | 333 | Facade9 | 324 | Facade9 | 185 |
| Facade10 | 165 | Facade10 | 916 | Facade10 | 370 | Facade10 | 370 |
| Facade11 | 33 | Facade11 | 166 | Facade11 | 92 | Facade11 | 185 |
| Facade12 | 66 | Facade12 | 166 | Facade12 | 0 | Facade12 | 92 |
| roof | 2058 | | | | | | |

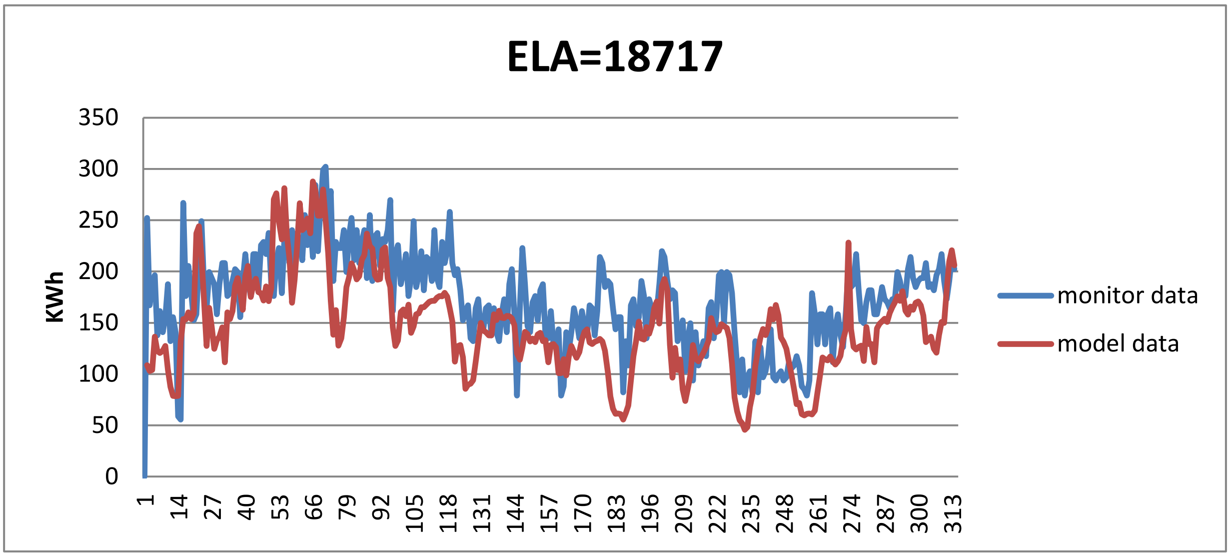


$\sqrt{\text{MES}}=43$

4. Total ELA=22460cm2at4pa

| Basement | ELA(cm2) | First floor | ELA(cm2) | Second floor | ELA(cm2) | Third floor | ELA(cm2) |
|---|---|---|---|---|---|---|---|
| Facade1 | 278 | Facade1 | 700 | Facade1 | 389 | Facade1 | 389 |
| Facade2 | 159 | Facade2 | 2314 | Facade2 | 2517 | Facade2 | 1433 |
| Facade3 | 278 | Facade3 | 700 | Facade3 | 389 | Facade3 | 389 |
| Facade4 | 79 | Facade4 | 200 | Facade4 | 111 | Facade4 | 111 |
| Facade5 | 40 | Facade5 | 200 | Facade5 | 0 | Facade5 | 111 |
| Facade6 | 357 | Facade6 | 1400 | Facade6 | 444 | Facade6 | 444 |
| Facade7 | 40 | Facade7 | 700 | Facade7 | 389 | Facade7 | 222 |
| Facade8 | 159 | Facade8 | 400 | Facade8 | 222 | Facade8 | 222 |
| Facade9 | 40 | Facade9 | 400 | Facade9 | 389 | Facade9 | 222 |
| Facade10 | 198 | Facade10 | 1100 | Facade10 | 444 | Facade10 | 444 |
| Facade11 | 40 | Facade11 | 200 | Facade11 | 111 | Facade11 | 222 |
| Facade12 | 79 | Facade12 | 200 | Facade12 | 0 | Facade12 | 111 |
| roof | 2472 | | | | | | |

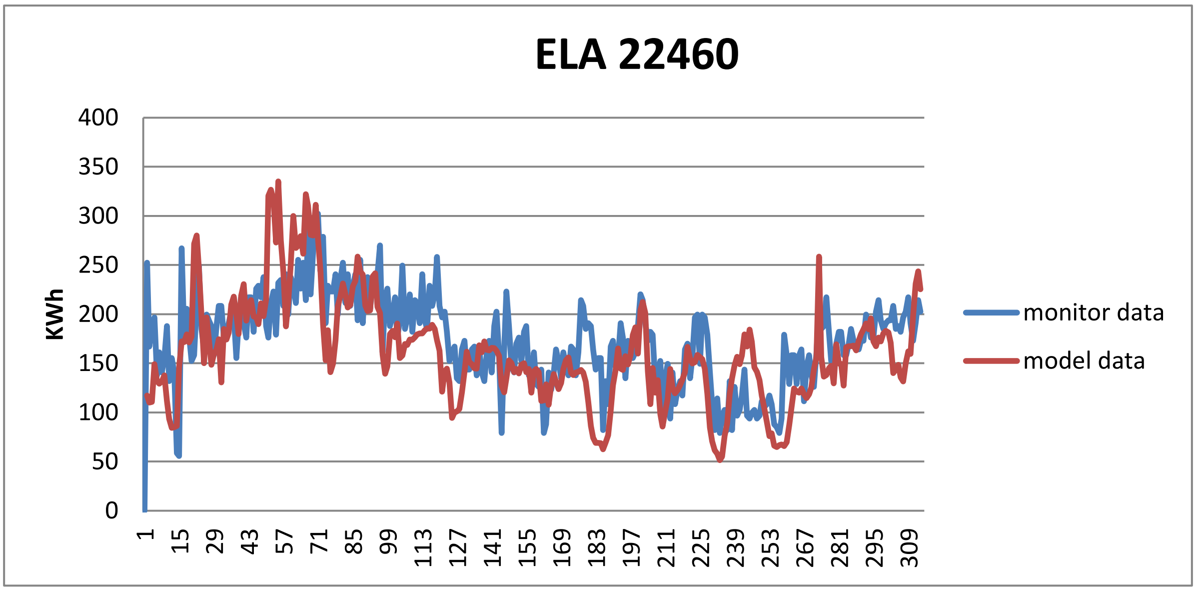


$\sqrt{MES}$=40.14

5. Total ELA=23437cm2at4pa

| Basement | ELA(cm2) | First floor | ELA(cm2) | Second floor | ELA(cm2) | Third floor | ELA(cm2) |
|---|---|---|---|---|---|---|---|
| Facade1 | 290 | Facade1 | 730 | Facade1 | 406 | Facade1 | 406 |
| Facade2 | 166 | Facade2 | 2415 | Facade2 | 2626 | Facade2 | 1496 |
| Facade3 | 290 | Facade3 | 730 | Facade3 | 406 | Facade3 | 406 |
| Facade4 | 83 | Facade4 | 209 | Facade4 | 116 | Facade4 | 116 |
| Facade5 | 41 | Facade5 | 209 | Facade5 | 0 | Facade5 | 116 |
| Facade6 | 373 | Facade6 | 1461 | Facade6 | 464 | Facade6 | 464 |
| Facade7 | 41 | Facade7 | 730 | Facade7 | 406 | Facade7 | 232 |
| Facade8 | 166 | Facade8 | 417 | Facade8 | 232 | Facade8 | 232 |
| Facade9 | 41 | Facade9 | 417 | Facade9 | 406 | Facade9 | 232 |
| Facade10 | 207 | Facade10 | 1148 | Facade10 | 464 | Facade10 | 464 |
| Facade11 | 41 | Facade11 | 209 | Facade11 | 116 | Facade11 | 232 |
| Facade12 | 83 | Facade12 | 209 | Facade12 | 0 | Facade12 | 116 |
| roof | 2580 | | | | | | |

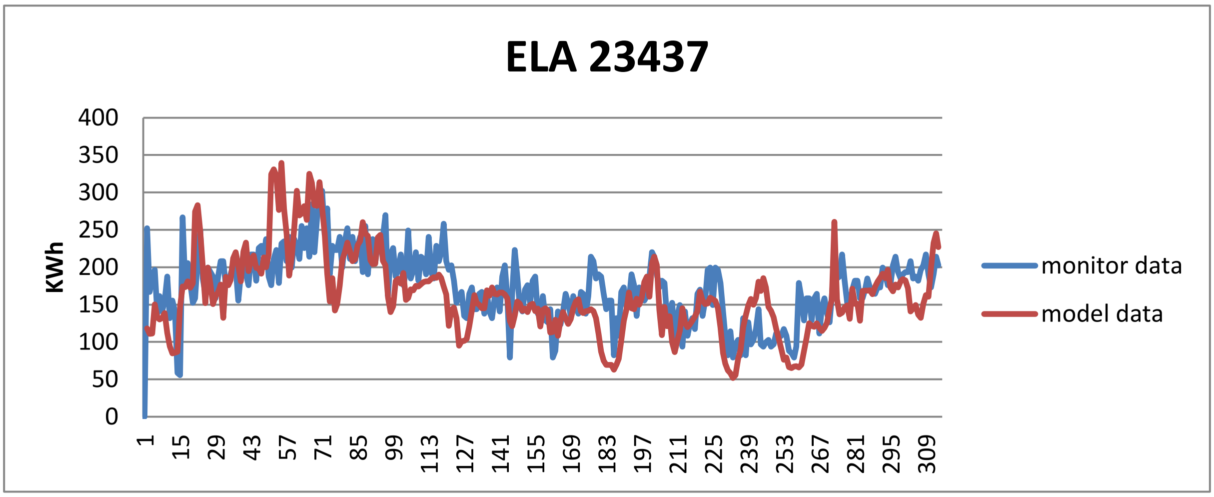


$\sqrt{MES}$=40.21

6. Total ELA=24502cm2at4pa

| Basement | ELA(cm2) | First floor | ELA(cm2) | Second floor | ELA(cm2) | Third floor | ELA(cm2) |
|---|---|---|---|---|---|---|---|
| Facade1 | 303 | Facade1 | 764 | Facade1 | 424 | Facade1 | 424 |
| Facade2 | 173 | Facade2 | 2525 | Facade2 | 2745 | Facade2 | 1564 |
| Facade3 | 303 | Facade3 | 764 | Facade3 | 424 | Facade3 | 424 |
| Facade4 | 87 | Facade4 | 218 | Facade4 | 121 | Facade4 | 121 |
| Facade5 | 43 | Facade5 | 218 | Facade5 | 0 | Facade5 | 121 |
| Facade6 | 390 | Facade6 | 1527 | Facade6 | 485 | Facade6 | 485 |
| Facade7 | 43 | Facade7 | 764 | Facade7 | 424 | Facade7 | 242 |
| Facade8 | 173 | Facade8 | 436 | Facade8 | 242 | Facade8 | 242 |
| Facade9 | 43 | Facade9 | 436 | Facade9 | 424 | Facade9 | 242 |
| Facade10 | 216 | Facade10 | 1200 | Facade10 | 485 | Facade10 | 485 |
| Facade11 | 43 | Facade11 | 218 | Facade11 | 121 | Facade11 | 242 |
| Facade12 | 87 | Facade12 | 218 | Facade12 | 0 | Facade12 | 121 |
| roof | 2697 | | 0 | | | | |

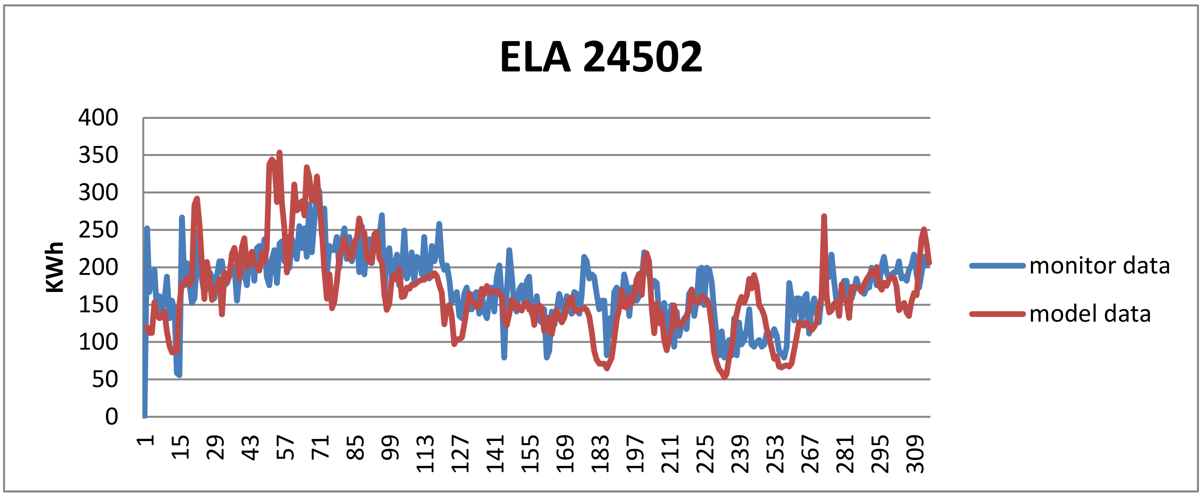


$\sqrt{MES}$=40.68

7.  Total ELA=25569cm2at4pa

| Basement | ELA(cm2) | First floor | ELA(cm2) | Second floor | ELA(cm2) | Third floor | ELA(cm2) |
|---|---|---|---|---|---|---|---|
| Facade1 | 317 | Facade1 | 800 | Facade1 | 444 | Facade1 | 444 |
| Facade2 | 181 | Facade2 | 2645 | Facade2 | 2876 | Facade2 | 1638 |
| Facade3 | 317 | Facade3 | 800 | Facade3 | 444 | Facade3 | 444 |
| Facade4 | 91 | Facade4 | 229 | Facade4 | 127 | Facade4 | 127 |
| Facade5 | 45 | Facade5 | 229 | Facade5 | 0 | Facade5 | 127 |
| Facade6 | 408 | Facade6 | 1600 | Facade6 | 508 | Facade6 | 508 |
| Facade7 | 45 | Facade7 | 800 | Facade7 | 444 | Facade7 | 254 |
| Facade8 | 181 | Facade8 | 457 | Facade8 | 254 | Facade8 | 254 |
| Facade9 | 45 | Facade9 | 457 | Facade9 | 444 | Facade9 | 254 |
| Facade10 | 227 | Facade10 | 1257 | Facade10 | 508 | Facade10 | 508 |
| Facade11 | 45 | Facade11 | 229 | Facade11 | 127 | Facade11 | 254 |
| Facade12 | 91 | Facade12 | 229 | Facade12 | 0 | Facade12 | 127 |
| roof | 2825 | | | | | | |

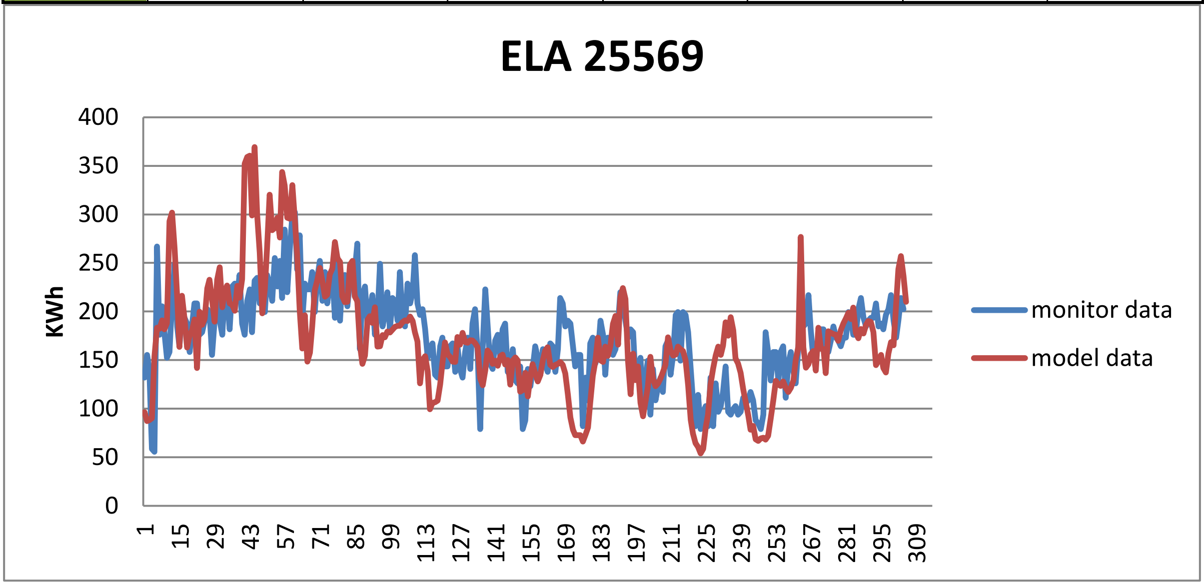


$\sqrt{MES}$=41.64

8.  Total ELA=26953cm2at4pa

| Basement | ELA(cm2) | First floor | ELA(cm2) | Second floor | ELA(cm2) | Third floor | ELA(cm2) |
|---|---|---|---|---|---|---|---|
| Facade1 | 333 | Facade1 | 840 | Facade1 | 467 | Facade1 | 467 |
| Facade2 | 190 | Facade2 | 2777 | Facade2 | 3020 | Facade2 | 1720 |
| Facade3 | 333 | Facade3 | 840 | Facade3 | 467 | Facade3 | 467 |
| Facade4 | 95 | Facade4 | 240 | Facade4 | 133 | Facade4 | 133 |
| Facade5 | 48 | Facade5 | 240 | Facade5 | 0 | Facade5 | 133 |
| Facade6 | 429 | Facade6 | 1680 | Facade6 | 533 | Facade6 | 533 |
| Facade7 | 48 | Facade7 | 840 | Facade7 | 467 | Facade7 | 267 |

| | | | | | | | |
|---|---|---|---|---|---|---|---|
| Facade8 | 190 | Facade8 | 480 | Facade8 | 267 | Facade8 | 267 |
| Facade9 | 48 | Facade9 | 480 | Facade9 | 467 | Facade9 | 267 |
| Facade10 | 238 | Facade10 | 1320 | Facade10 | 533 | Facade10 | 533 |
| Facade11 | 48 | Facade11 | 240 | Facade11 | 133 | Facade11 | 267 |
| Facade12 | 95 | Facade12 | 240 | Facade12 | 0 | Facade12 | 133 |
| roof | 2967 | | | | | | |

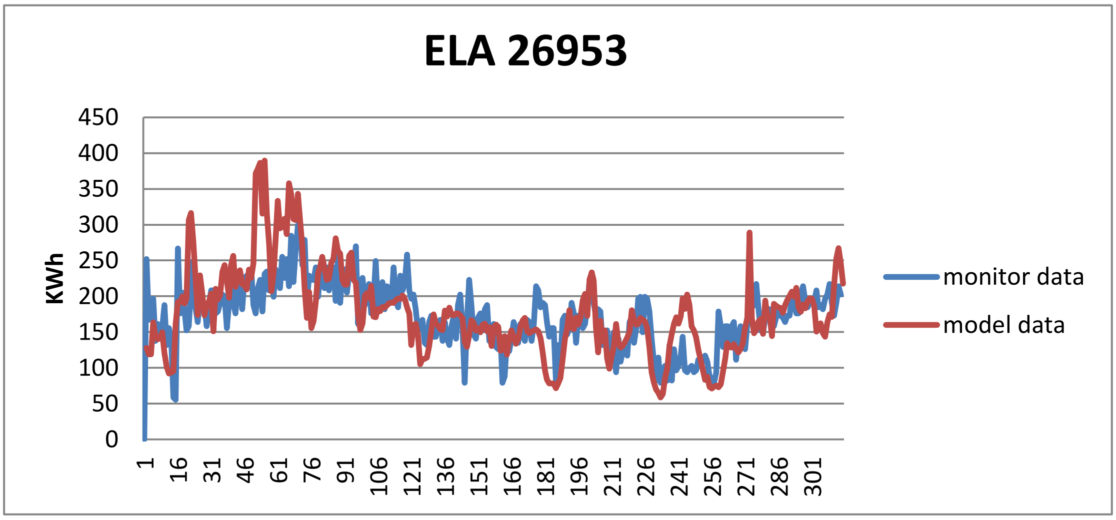


$\sqrt{\text{MES}}$=43.36

9. Total ELA=29403cm2at4pa

| Basement | ELA(cm2) | First floor | ELA(cm2) | Second floor | ELA(cm2) | Third floor | ELA(cm2) |
|---|---|---|---|---|---|---|---|
| Facade1 | 364 | Facade1 | 916 | Facade1 | 509 | Facade1 | 509 |
| Facade2 | 208 | Facade2 | 3030 | Facade2 | 3295 | Facade2 | 1876 |
| Facade3 | 364 | Facade3 | 916 | Facade3 | 509 | Facade3 | 509 |
| Facade4 | 104 | Facade4 | 262 | Facade4 | 145 | Facade4 | 145 |
| Facade5 | 52 | Facade5 | 262 | Facade5 | 0 | Facade5 | 145 |
| Facade6 | 468 | Facade6 | 1833 | Facade6 | 582 | Facade6 | 582 |
| Facade7 | 52 | Facade7 | 916 | Facade7 | 509 | Facade7 | 291 |
| Facade8 | 208 | Facade8 | 524 | Facade8 | 291 | Facade8 | 291 |
| Facade9 | 52 | Facade9 | 524 | Facade9 | 509 | Facade9 | 291 |
| Facade10 | 260 | Facade10 | 1440 | Facade10 | 582 | Facade10 | 582 |
| Facade11 | 52 | Facade11 | 262 | Facade11 | 145 | Facade11 | 291 |
| Facade12 | 104 | Facade12 | 262 | Facade12 | 0 | Facade12 | 145 |
| roof | 3236 | | | | | | |

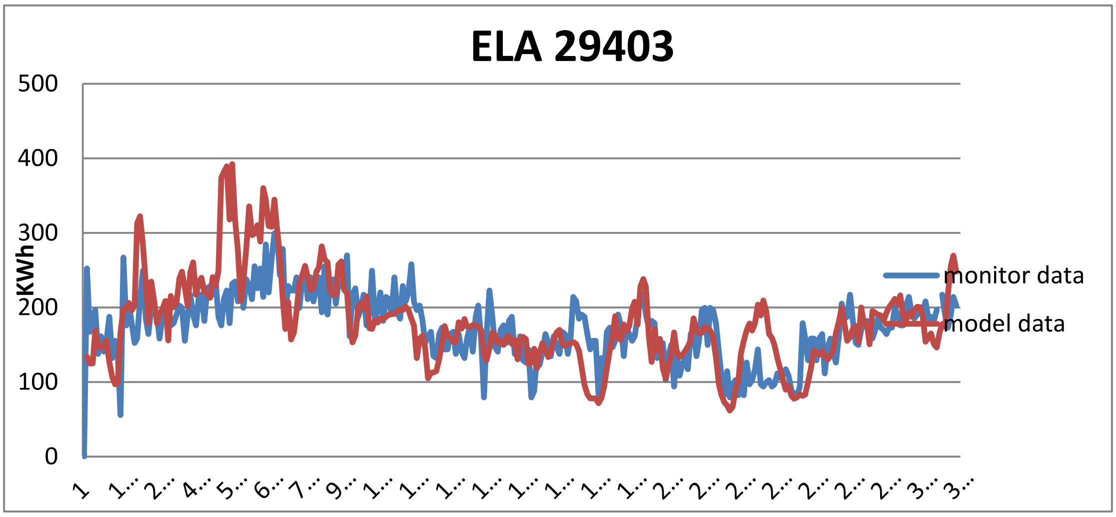


$\sqrt{MES}$=44.78

10. Total ELA=32343cm2at4pa

| Basement | ELA(cm2) | First floor | ELA(cm2) | Second floor | ELA(cm2) | Third floor | ELA(cm2) |
|---|---|---|---|---|---|---|---|
| Facade1 | 400 | Facade1 | 1008 | Facade1 | 560 | Facade1 | 560 |
| Facade2 | 229 | Facade2 | 3332.8 | Facade2 | 3624 | Facade2 | 2064 |
| Facade3 | 400 | Facade3 | 1008 | Facade3 | 560 | Facade3 | 560 |
| Facade4 | 114 | Facade4 | 288 | Facade4 | 160 | Facade4 | 160 |
| Facade5 | 57 | Facade5 | 288 | Facade5 | 0 | Facade5 | 160 |
| Facade6 | 514 | Facade6 | 2016 | Facade6 | 640 | Facade6 | 640 |
| Facade7 | 57 | Facade7 | 1008 | Facade7 | 560 | Facade7 | 320 |
| Facade8 | 229 | Facade8 | 576 | Facade8 | 320 | Facade8 | 320 |
| Facade9 | 57 | Facade9 | 576 | Facade9 | 560 | Facade9 | 320 |
| Facade10 | 286 | Facade10 | 1584 | Facade10 | 640 | Facade10 | 640 |
| Facade11 | 57 | Facade11 | 288 | Facade11 | 160 | Facade11 | 320 |
| Facade12 | 114 | Facade12 | 288 | Facade12 | 0 | Facade12 | 160 |
| roof | 3560 | | | | | | |

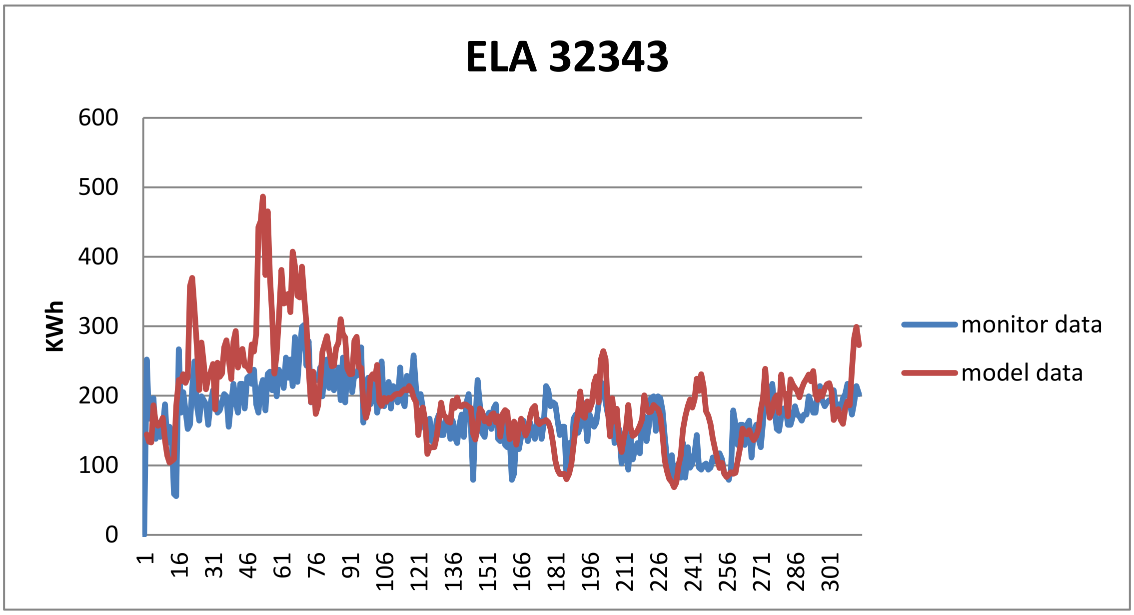


$\sqrt{\text{MES}}=56.77$

# REFERENCES


[1] Sherman, Max H., and Jennifer A. McWilliams. *"Air Leakage of US Homes: Model Prediction."* Proc. 10th Conf, Thermal Perf, Ext Env of Buildings, LBNL-62078. 2007

[2] Hyun. S, Park C, Augenbroe, G. "*Analysis of uncertainty in natural ventilation predictions of high-rise apartment buildings*", Building services Engineering Research & Technology. November 2008;29(4):311

[3] Handbook, A. S. H. R. A. E. (2009). Fundamentals. Chapter16 American Society of Heating, Refrigerating and Air-Conditioning Engineers, Inc., Atlanta GA

[4] Handbook, A. S. H. R. A. E. (2009). Fundamentals. Chapter 13 American Society of Heating, Refrigerating and Air-Conditioning Engineers, Inc., Atlanta GA

[5] Walton, G. N., & Dols, W. S. (2005). CONTAM 2.4 user guide and program documentation. National Institute of Standards and Technology, NISTIR, 7251

[6] K Gowri, D Winiarski, R Jarnagin, "*Infiltration Modeling Guidelines for Commercial Building Energy Analysis*", Prepared for the U.S Department of Energy

[7] Wilcox, Stephen, and William Marion. Users manual for TMY3 data sets. National Renewable Energy Laboratory, 2008.

[8] Y. Heo, R Choudhary, G.A.Augenbroe, "*Calibration of building energy models for retrofit analysis under uncertainty"*, Journal of the Energy and Savings, 47(2012)550-560

[9] M.C. Kennedy, A. O'Hagan, "*Bayesian calibration of computer models*", Journal of the Royal Statistical Society, Series B 63 (2001) 425–464.